Progress in Energy

OPEN ACCESS

RECEIVED
1 July 2020

ACCEPTED FOR PUBLICATION
14 January 2021

PUBLISHED
12 March 2021

TOPICAL REVIEW

Progress and prospects of thermo-mechanical energy storage—a critical review

Andreas V Olympios[1], Joshua D McTigue[2], Pau Farres-Antunez[3], Alessio Tafone[4], Alessandro Romagnoli[4,5], Yongliang Li[6], Yulong Ding[6], Wolf-Dieter Steinmann[7], Liang Wang[8], Haisheng Chen[8] and Christos N Markides[1,*]

[1] Clean Energy Processes (CEP) Laboratory, Department of Chemical Engineering, Imperial College London, London SW7 2AZ, United Kingdom
[2] National Renewable Energy Laboratory, 15013 Denver West Parkway, Golden, CO 80401, United States of America
[3] Department of Engineering, University of Cambridge, Cambridge CB2 1PZ, United Kingdom
[4] Energy Research Institute @ NTU (ERI@N), Nanyang Technological University, 1 Cleantech Loop 637141, Singapore
[5] School of Mechanical and Aerospace Engineering, Nanyang Technological University, 50 Nanyang Avenue 639798, Singapore
[6] Birmingham Centre for Energy Storage & School of Chemical Engineering, University of Birmingham, Edgbaston, Birmingham B15 2TT, United Kingdom
[7] German Aerospace Center (DLR), Institute of Engineering Thermodynamics, Pfaffenwaldring 38-40, Stuttgart 70569, Germany
[8] Institute of Engineering Thermophysics, Chinese Academy of Sciences (CAS), Beijing 100190, People's Republic of China
[*] Author to whom any correspondence should be addressed.

E-mail: c.markides@imperial.ac.uk

Keywords: thermo-mechanical energy storage (TMES), compressed-air energy storage (CAES), pumped-thermal electricity storage (PTES), liquid-air energy storage (LAES)

Abstract

The share of electricity generated by intermittent renewable energy sources is increasing (now at 26% of global electricity generation) and the requirements of affordable, reliable and secure energy supply designate grid-scale storage as an imperative component of most energy transition pathways. The most widely deployed bulk energy storage solution is pumped-hydro energy storage (PHES), however, this technology is geographically constrained. Alternatively, flow batteries are location independent and have higher energy densities than PHES, but remain associated with high costs and short lifetimes, which highlights the importance of developing and utilizing additional larger-scale, longer-duration and long-lifetime energy storage alternatives. In this paper, we review a class of promising bulk energy storage technologies based on thermo-mechanical principles, which includes: compressed-air energy storage, liquid-air energy storage and pumped-thermal electricity storage. The thermodynamic principles upon which these thermo-mechanical energy storage (TMES) technologies are based are discussed and a synopsis of recent progress in their development is presented, assessing their ability to provide reliable and cost-effective solutions. The current performance and future prospects of TMES systems are examined within a unified framework and a thermo-economic analysis is conducted to explore their competitiveness relative to each other as well as when compared to PHES and battery systems. This includes carefully selected thermodynamic and economic methodologies for estimating the component costs of each configuration in order to provide a detailed and fair comparison at various system sizes. The analysis reveals that the technical and economic characteristics of TMES systems are such that, especially at higher discharge power ratings and longer discharge durations, they can offer promising performance (round-trip efficiencies higher than 60%) along with long lifetimes (>30 years), low specific costs (often below 100 \$ kWh^{-1}), low ecological footprints and unique sector-coupling features compared to other storage options. TMES systems have significant potential for further progress and the thermo-economic comparisons in this paper can be used as a benchmark for their future evolution.

Abbreviations

A-CAES	adiabatic compressed-air energy storage
AA-CAES	advanced adiabatic compressed-air energy storage
CAES	compressed-air energy storage
CHEST	compressed-heat energy storage
CHP	combined heat and power
CSP	concentrated solar power
D-CAES	diabatic compressed-air energy storage
HGCS	high-grade cold storage
HGWS	high-grade warm storage
I-CAES	isothermal compressed-air energy storage
IA-CAES	isobaric-adiabatic compressed-air energy storage
IEA	International Energy Association
LAES	liquid-air energy storage
LTA-CAES	low-temperature adiabatic compressed-air energy storage
ORC	organic Rankine cycle
PCM	phase-change material
PHES	pumped-hydro energy storage
PHP	power-to-heat-to-power
PTES	pumped-thermal electricity storage
PV	photovoltaic
SC-CAES	supercritical compressed-air energy storage
sCO_2	supercritical carbon dioxide
TES	thermal energy storage
TRL	technology readiness level
UW-CAES	underwater compressed-air energy storage
VRB	vanadium redox flow batteries
WEC	World Energy Council

1. Introduction

Advances to renewable energy technologies have led to continued cost reductions and performance improvements [1]. PV cells and wind generation are continuing to gain momentum [2, 3] and a possible transition towards electrification of various industries (e.g. electric heating in homes, electric cars, increasing cooling loads in developing countries) will increase electricity demand [4]. Limiting global emissions entails major challenges, requiring the contribution of critical technologies [5], while the unpredictability and seasonal variation of energy generation and demand present a great pressure to develop solutions that can ensure the reliability and stability of a renewable energy system [6]. In this effort, grid-scale energy storage is recognized as an imperative component of the energy transition [7], with both the IEA and WEC estimating that meeting global targets will require a world energy storage capacity in excess of 250 GW by 2030 [8, 9].

Energy storage refers to the process of converting energy from one form (often electrical energy) to a form that can be stored and then converted back to its initial form when required. From a country-wide energy system's perspective, storage should provide reliability and security of energy supply. Grid-scale storage therefore requires two main characteristics: (a) the ability to time-shift energy provision over daily time periods (in the order of hours); and (b) the ability to supply high power (in the order of MW). In today's power grids, PHES accounts for the majority of energy storage capacity with more than 96% of the total world capacity [10]. PHES systems use gravitational force to generate electricity, by pumping water from a low-elevation to a high-elevation reservoir and then releasing it through turbines to produce electricity when required. They have energy capital costs that vary between 5 and 100 $ kWh^{-1} [6] and they can retrieve about 80% of the energy put into storage [11]. The high discharge power ratings (100–1000 MW) and medium/long-discharge durations (4–12 h) of PHES systems makes them a suitable technology for grid-scale applications. However, PHES systems experience several challenges that limit the development of new plants: (a) they are location-constrained, since they require water availability and a significant geographical height difference between the potential reservoirs [8]; (b) they are associated with environmental concerns due to the requirement of a great deal of land and the ecological impact on ecosystems [12]; and (c) permitting and construction of these systems can take 3–5 years each [13].

Other potential solutions for medium/long-duration, medium/large-scale electricity storage are based on electrochemical storage. Despite being the most widely used electrochemical storage solution, lead-acid batteries have relatively short lifetimes with a limited number of cycles (~2000 cycles) and have found limited grid-scale application around the world [6]. Li-ion batteries, on the other hand, experience high energy capital costs (600–3800 $ kWh^{-1}) [6] when deployed for longer-duration electricity storage. An alternative

type of electrochemical storage is that of flow batteries, which are based largely on similar underlying electrochemical principles as conventional batteries, except that, instead of the energy being stored in the two electrodes that facilitate ion movement, energy is stored in external liquid-electrolyte solutions [11]. This means that the power and energy capacities are independent, providing flexibility of design, low self-discharge and longer life cycles [13]. The largest flow battery (200 MW, 800 MWh) is currently being constructed in Dalian, China [14]. Flow batteries can go beyond the, typically, 1–4 h discharge duration commonly associated with Li-ion batteries and can achieve efficiencies up to 85% [6]. VRBs are the most mature type and are associated with quick response (<0.001 s) and a large number of cycles compared to conventional batteries (>10 000), while the energy capital cost lies in the range 150–1000 \$ kWh^{-1} [11]. Flow batteries still face several challenges due to: (a) complicated system requirements (electrolytes are highly viscous) [15]; (b) narrow working temperatures [16]; (c) disposal or recycling issues [7]; and (d) shorter lifetimes [7].

The concept of TMES provides a promising alternative to PHES and flow batteries as a method of grid-scale, medium/long-duration energy storage. TMES refers to the process of storing energy based on transformations between thermal and mechanical energy [17]. Recently, significant advancements in TMES systems have illustrated their promising technical characteristics, while they also have fewer geographical constraints, lower environmental impact, long lifetime and entail unique features when compared to other grid-scale storage solutions: (a) they can be used to provide thermal energy along with electrical energy during discharging, which means they can be used for both provision of electricity and heat (district heating/industrial processes); (b) they can be integrated with other (e.g. waste, renewable) heat sources; and (c) they may be integrated into other power generation systems that involve thermal energy conversion.

The multiple ways in which energy storage can contribute towards an affordable and reliable energy system has led many authors to summarize the research in the field. Chen *et al* [7] provided an extensive critical review on the progress of electrical energy storage systems in 2009, capturing many types of electricity storage systems and comparing them in terms of their characteristics and potential applications. Luo *et al* [6] then delivered an updated picture on the state-of-the-art electricity storage systems, providing a clear overview of which options can be promising in different application areas. An overview of energy storage technologies was also provided by Gallo *et al* [11], which links how different technologies have a role to play in the energy transition. The mentioned studies, however, aimed to provide a broad overview of storage options, with low focus being placed on the various thermo-mechanical storage options. Georgiou *et al* [18] performed a comprehensive comparison between two TMES options (pumped-thermal and LAES systems), including preliminary estimates of their technoeconomic performance and feasibility, extending in [19] to assessments of the role and value of their deployment within whole-electricity systems. Benato *et al* [20] and Budt *et al* [21] produced reviews of pumped-thermal and CAES systems, respectively while Steinmann *et al* [22] compared five different PTES variants. However, a detailed review which assesses and compares all TMES options is lacking from literature.

In this paper we aim to review the recent progress in the advancement of thermo-mechanical bulk energy storage solutions. A wealth of concepts and configurations have been proposed in the literature. These resources are gathered, and key themes are described, providing a synopsis of the current development of these systems. The work involves performing, for the first time, a detailed thermo-economic analysis of the different thermo-mechanical options, making comparisons which have not been possible until this point. The technical and cost characteristics of the different options are assessed and compared to those of commercially available PHES systems and batteries. The framework involves assessing the performance and economic competitiveness of the different solutions at discharge power ratings and discharge durations as obtained from industrial applications and literature, but also at a range of different power ratings and durations, aiming for a holistic understanding of the evolution potential of TMES systems. In many cases, the insufficient documentation means that evaluating the cost of these options can be complicated. In order for the assessment to be as 'fair' as possible, thermodynamic and component-costing models of the main options are constructed using consistent performance metrics and cost correlations, where similar-type machines appearing in more than one of the considered systems are costed in the same way. The costing effort involves using mean estimates from multiple costing approaches based on the module costing technique, as in the work of Georgiou *et al* [18].

The paper begins with a technology landscape overview in section 2, and proceeds in section 3 to describe the operation principles and current research being conducted on TMES systems. The thermo-economic characteristics of different TMES options and their role as alternatives to PHES and battery systems are evaluated in section 4. Lastly, section 5 provides concluding remarks and a perspective for the future widespread deployment of these medium/large-scale, medium/long-duration energy storage systems.

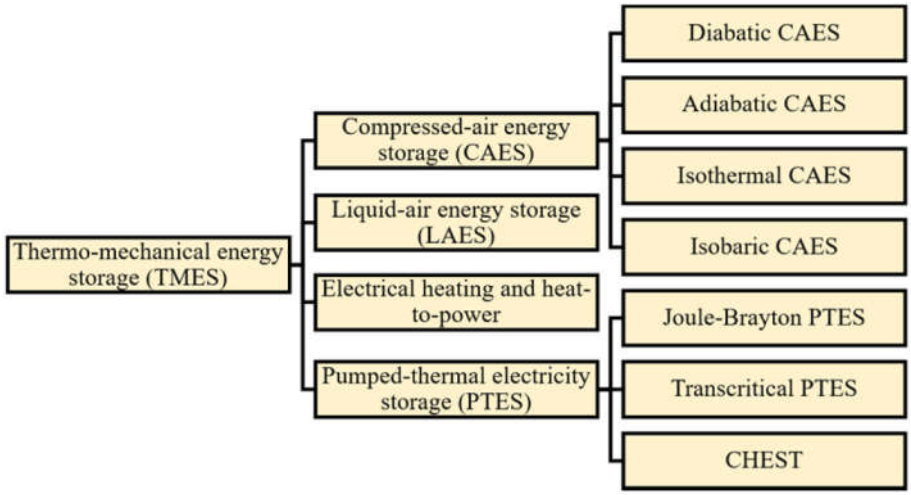

Figure 1. Overview of TMES options.

2. Technology landscape and evaluation criteria

This paper distinguishes between four main categories of TMES systems based on thermo-mechanical principles (figure 1):

(a) CAES systems, which involve storing energy in the form of high-pressure compressed air. These can be further divided into diabatic, adiabatic, isothermal and isobaric systems.
(b) LAES systems, which involve storing energy in the form of low-pressure liquefied air. Such systems can be standalone or involve polygeneration and hybrid configurations.
(c) PTES systems, which involve storing energy as a temperature difference between two reservoirs. These can be further divided into systems based on the Joule–Brayton cycle, transcritical cycles (such as the transcritical CO_2 cycle) and the CHEST concept. Each of these can in turn involve various polygeneration and hybrid configurations.
(d) Electrical heating and heat-to-power systems, also known as PHP systems [17], which involve charging a thermal energy store using electrical heating and discharging using a thermal cycle or in polygeneration mode, where some energy is released as thermal energy.

In this paper, the efficiency of the storage systems is often measured using the round-trip efficiency η_{RT}, defined as the ratio of the energy output during discharging W_{dis} to the energy input during charging W_{ch}:

$$\eta_{RT} = \frac{W_{dis}}{W_{ch}}. \tag{1}$$

It is noted, with respect to equation (1), that an assumption in the present work is made that conversion processes from electrical energy to mechanical work, and vice versa, have higher efficiencies, are faster and take place in smaller components than those associated with other processes in the technologies of interest, i.e. primarily those associated with mechanical- to thermal-energy conversion. In this case, overall technical/thermodynamic performance, e.g. as in equation (1), is determined by the latter processes, and reference to electrical energy and mechanical work are interchangeable in terms of performance. On the other hand, the cost of electrical to mechanical energy conversion components is accounted for explicitly when costing estimates are made in an effort to consider the technoeconomic performance of these technologies (see section 4.2.2).

A unique attribute of TMES systems is that the various flows of heat, cold and electricity facilitate integration with other energy processes. This means that TMES systems can be used as a flexible management tool for balancing available energy and demand. Comparing these advanced systems, however, which involve integration of heat sources and heat sinks, becomes more complicated. When heat is a useful output of the system, the requirements regarding the efficiencies and costs of system components are different, and in these cases, the round-trip efficiency becomes less relevant.

Furthermore, in this work, the power density and the energy density of a technology are defined as the discharge power rating divided by the total volume the technology occupies, and the total energy stored

Table 1. Commercial CAES plants in operation [23, 24].

Name	Type	Discharge power rating (MW)	Storage type	Storage volume (m^3)	Cycle efficiency (%)
Huntorf	D-CAES	321	Salt cavern	310 000	42
McIntosh	D-CAES with recuperation	110	Salt cavern	532 000	54

(a) (b)

Figure 2. (a) External view; and (b) machine hall of the Huntorf CAES plant. (a) Reproduced from [25]. CC BY 4.0. (b) Reprinted from [21], Copyright (2016), with permission from Elsevier.

divided by the total volume the technology occupies, respectively. All cost comparisons in this paper are provided in USD ($). Electrical heating and heat-to-power systems have relatively low expected round-trip efficiencies and limited available information [17], therefore they are briefly discussed in section 3 but are not included in the thermo-economic analysis of section 4.

3. Thermo-mechanical energy storage systems

This section provides a description of TMES systems and an overview of their underpinning principles of operation. This includes technology variants, their maturity, target scales, advantages/disadvantages, and recent research and developments.

3.1. Compressed-air energy storage

CAES refers to electrical energy converted to potential energy in the form of compressed air, which is converted back to electricity upon demand. The concept of CAES was first proposed in Gay's patent [26] as early as in the 1940s. CAES technology had been developed for the need of load-peaking and black start of the power grid until 1970s. As listed in table 1, two commercial CAES plants have been constructed in Huntorf, Germany in 1978 (figure 2) and McIntosh, USA in 1991, which are currently in operation [6, 7, 21]. Other countries such as UK, Japan, China and Canada have been active in developing CAES technology.

In the case of CAES systems, a measure of efficiency often used (except round-trip efficiency) is cycle efficiency, which is defined as the ratio of the electrical energy output during discharging W_{dis} to the sum of the electrical energy input W_{ch} and thermal energy of fossil fuel used during charging Q_{fuel}:

$$\eta_{cycle} = \frac{W_{dis}}{W_{ch}} + Q_{fuel}. \tag{2}$$

Existing CAES systems can be divided into three main categories according to technological features: (a) D-CAES; (b) A-CAES; and (c) I-CAES. This section presents a brief overview of advances in these variants, as well as in commonly proposed isobaric CAES systems. Research and development into CAES systems and their key components have been reviewed in detail in [6, 7, 21, 27].

3.1.1. Diabatic CAES

The conventional D-CAES is the primary type of CAES systems derived from a gas turbine cycle. A diagram of the main components of the conventional system is displayed in figure 3. The system involves compressors, expanders, intercoolers and air storage. During the charging period, ambient air is compressed in an air-tight space such as underground cavern driven by compressors. During compression, heat is wasted to the ambient through intercoolers. During the discharging period, compressed air is mixed with fuel (external heat source) and combusted to drive expanders and generate electricity.

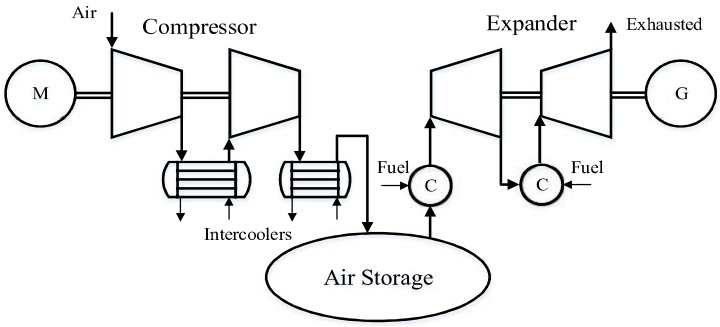

Figure 3. Schematic of a D-CAES system illustrating the processes of: (a) compression; (b) release of heat to ambient air; (c) air storage; (d) fuel addition; and (e) expansion.

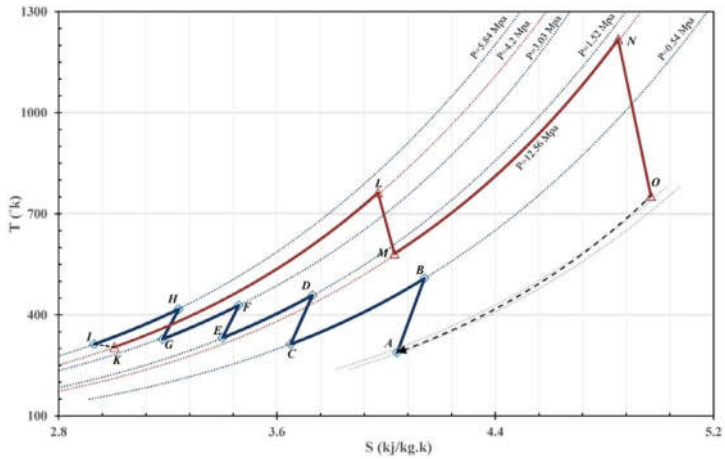

Figure 4. *T–s* diagram of charging and discharging of the Huntorf plant, as modelled in and reprinted from [28], Copyright (2020), with permission from Elsevier.

The first D-CAES plant put into use is the Huntorf plant, located in Germany [23], which has a storage pressure of 44–70 bars and an air-storage capacity of 310 000 m^3 (solution-mined salt caverns), being able to provide, at full load, 290 MW of electricity for 4 h with a total cycle efficiency of 42%. An idealized *T–s* diagram of the Huntorf plant is shown in figure 4, including the compression (A → I) and expansion (I → O) processes, taken from the work of Jafarizadehah *et al* [28]. The second D-CAES plant has been in operation at McIntosh since 1991 [21], which has an air-storage capacity of 532 000 m^3 (solution-mined salt caverns) and can provide, at full load, 110 MW of electricity for 26 h. The McIntosh plant recovers the residual heat from the exhaust of the low-pressure expander while charging, using it to preheat the high-pressure gas during the discharging process, hence the cycle efficiency is increased to 54%. Besides the two commercial D-CAES plants, small experimental D-CAES facilities have been also constructed. For example, in Sesta, Italy, a 20 MW D-CAES test facility has been built in a fractured-rock aquifer by Italian public utilities (ENEL) [24], and a 2 MW, 4 h D-CAES pilot facility has been constructed at Kamisunagawa, Japan [29].

D-CAES has several disadvantages: (a) significant amount of compression heat loss; (b) requirement of fossil fuels which leads to inevitable emissions; and (c) requirement of suitable geological conditions. Denholm [30] presented that using biomass as the fuel of CAES can reduce the related net-carbon emissions and thus increase the proportion of renewable energy in the power grid. Safaei *et al* [31, 32] proposed and evaluated a distributed CAES system, where the compression heat is recovered to provide low-grade heat. They found that for fuel prices higher than 7.6 \$ GJ^{-1} and pipeline lengths lower than 50 km, the distributed CAES system can be economically advantageous and environmentally friendly.

3.1.2. Adiabatic CAES

In order to overcome the shortcomings of the conventional D-CAES system, the concept of A-CAES was proposed in the 1980s. The key feature of this system is that it stores the heat generated by compression in a TES vessel, reusing the stored heat to preheat pressurized air in the generation process, thus reducing or even eliminating the consumption of natural gas. A-CAES has the advantages of high efficiency, zero carbon

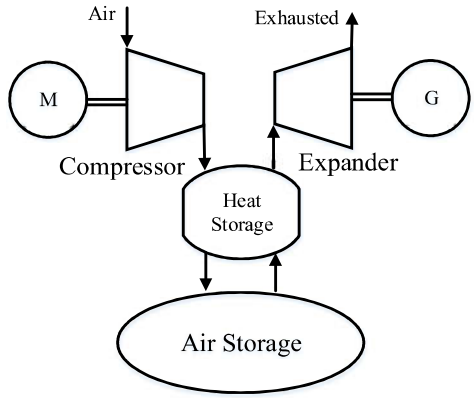

Figure 5. Schematic of a A-CAES system illustrating the processes of: (a) compression; (b) heat storage; (c) air storage; (d) reuse of stored heat; and (e) expansion.

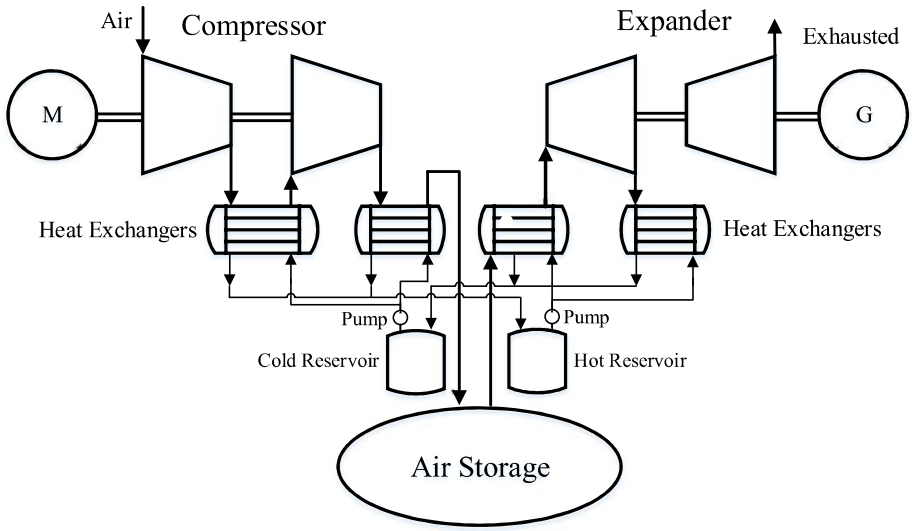

Figure 6. Schematic of a LTA-CAES system illustrating the processes of: (a) compression; (b) heat storage through multiple heat exchangers in cold and hot reservoirs (c) air storage; (d) reuse of stored heat; and (e) expansion.

emissions and less geographical restrictions. Depending on the system, the A-CAES process can involve storage at a large range of temperatures. The concept of high-temperature A-CAES, also referred as AA-CAES, involves single-stage and high-temperature (~570 °C) TES. The latter system was firstly developed in the project 'ADELE' [21, 33]. A diagram of the main components of this system is shown in figure 5. Barbour *et al* [34] performed a detailed thermodynamic analysis on an AA-CAES system with a packed-bed TES and obtained a continuous cycle efficiency of ~71%. Sciacovelli *et al* [35] developed a dynamic and off-design performance model of an A-CAES plant, and their analysis indicates that the A-CAES system cycle efficiency can reach 70%, while the thermal storage efficiency (heat energy output during discharging over heat energy input during charging) reaches 95%.

In order to overcome the technical difficulties associated with the high temperature in the compressor and TES of AA-CAES systems, an LTA-CAES system has been developed [36, 37], demonstrating that fast cycling capabilities improve profitability. Hartmann *et al* [36] reported that an A-CAES system with a two-stage compression and one-stage relaxation achieves the highest cycle efficiency which is between 49% and 61%. Luo *et al* [38] found that the round-trip efficiency of LTA-CAES can be up to 68%. Multiple heat exchangers are needed for the LTA-CAES and the influence of the heat exchanger's effectiveness and pressure loss on the efficiency has been analysed by Yang *et al* [39]. A schematic of the main components of LTA-CAES appears in figure 6.

Improved technology for A-CAES systems has emerged. Liu and Wang [40] modified A-CAES systems to produce electricity, heating and cooling simultaneously with a 3% improvement in exergy efficiency (total exergy output during discharging over total exergy input during charging). For the off-design performance of the A-CAES system, Guo *et al* [41] proposed and compared two operational modes of LTA-CAES: (a)

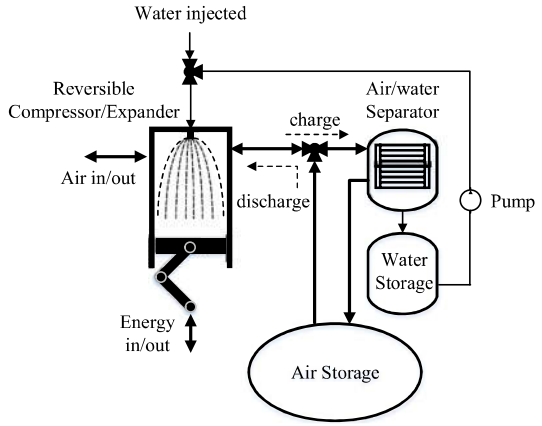

Figure 7. Schematic of a closed I-CAES system illustrating the processes of isothermal compression (cold liquid is injected into the cylinder) and isothermal expansion (warm liquid is re-injected into the cylinder). The storage process involves a machine that can be reversed in order to act as both a compressor (charging) and an expander (discharging) at different times.

optimizing the variable inlet guide vane rotation angle; and (b) achieving equal pressure ratio, providing support for the design of CAES systems. Peng *et al* [42] reported that the cycle efficiency of the A-CAES combined with a packed-bed TES system is about 50%, which is improved to 57% with heat recuperation. Guo *et al* [43] found that the cycle efficiency of A-CAES system can be improved by more than 3% when introducing an ejector (a device that produces middle pressure air flow by mixing high-pressure and low-pressure air flows) to assist the pressure regulation process of compressed air and thus reduce energy loss.

3.1.3. Isothermal CAES

I-CAES is a new kind of CAES technology which attempts to achieve isothermal compression during charging and isothermal expansion during discharging by continuous effective heat transfer using a water spray or foams. Theoretically, the I-CAES system has an estimated round-trip efficiency of 80% [44]. In 2013, the company SustainX built the first 1.5 MW I-CAES demonstration plant [45].

The concept of I-CAES was first implemented in hydro-pneumatic energy storage [21], where air compression is done using a liquid piston. There are currently open and closed I-CAES systems [46]. In a closed I-CAES system (figure 7), the liquid is injected into the cylinder of the reciprocating compressor during the charging stage in the form of small droplets or foam, and is blended with the compressed air; it is then collected into a liquid storage reservoir after separation. During discharging, the compressed air is re-blended with warm re-injected liquid in the reciprocating cylinder, driving the piston to produce power (electricity). The open I-CAES system avoids the shortcomings of the low energy density of the closed systems, using two alternating cylinders to achieve a cyclic supply and release of the air. The concept of using the ocean as a heat source/sink has been proposed [47, 48], which involves the utilisation of seawater in the liquid piston for air compression. In this 'open accumulator', the compressed space has a high surface area, which makes high heat transfer and therefore high efficiency possible. The concept of isothermal compression/expansion has been considered into ocean CAES systems in [49, 50].

The main challenge of I-CAES is to obtain isothermal or quasi-isothermal compression and expansion. One strategy is to spray tiny drops of water into the pistons [51–54]. Coney *et al* [51] developed a reciprocating air compressor which can achieve quasi-isothermal compression by injecting water into the cylinder where air is kept below 100 °C. Zhang *et al* [52] designed a specific expander for I-CAES, demonstrating that for the same air mass flowrate, spraying water droplets into the cylinder results in an enhancement of the specific work generation and a reduction in the cylinder size. Iglesias *et al* [53] described the injection of water into the co-rotating scroll compressor-expander. By extrapolating the results from experiments, they showed that the overall turbine efficiency can reach about 70%–75% with water injection. The use of pre-mixed foam to improve heat transfer efficiency was proposed by McBride *et al* [54]. Furthermore, the use of a liquid piston combined with a solid piston actuated by a hydraulic intensifier demonstrated a rise in overall pump efficiency from 27% to 65% at the optimum intensifier ratio [55]. Heidari *et al* [56] investigated a novel finned compressor with increased heat transfer area and coefficient, achieving an increase of more than 20% in exergetic efficiency compared to the classic piston. Lastly, Castellani *et al* [57] proposed the use of PCM in the isothermal process, showing an increase in expansion work between 4% and 9%.

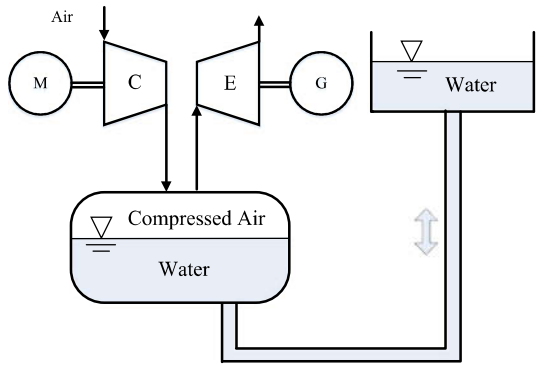

Figure 8. Isobaric CAES system with compensating water column.

3.1.4. Isobaric CAES

Compressed air is commonly stored in caverns and pressure vessels at constant volume, however, the container pressure decreases during discharging. Isobaric CAES has been proposed so that the compressed air is instead stored in a container kept at nearly-constant pressure, which can happen by utilizing a water column either from a surface reservoir so as to displace compressed air (figure 8) or in the case of an underground cavern by using a brine shuttle pond at the surface [58]. In order to eliminate the restrictions of geographical conditions, Kim and Favrat [59] proposed an IA-CAES system combined with PHES, where the air-storage pressure is kept constant by pumping or motoring water to and from hydraulic accumulators. Mazloum *et al* [60] carried out the dynamic modelling of an IA-CAES system, predicting a round-trip efficiency of 54%.

Another form of isobaric CAES involves the utilisation of underwater air bags instead of a cavern. UW-CAES systems highly loosen geographical constraints. The company Hydrostor launched a successful pilot plant of an UW-CAES system in 2015 [61]. The underground air bags, which are often called 'Energy Bags', are cable-reinforced fabric vessels anchored to the sea. Details about the structure are found in the work of Pimm *et al* [62], which shows results of tank-based testing but also off-shore testing, demonstrating that underground air bags can potentially provide a reliable method for high-pressure air storage. In the work of Cheung *et al* [63], the influence of pipe diameter, expander/compressor efficiencies and air storage depth on the round-trip efficiency of UW-CAES is studied, reporting that at baseline configuration, the latter is equal to about 56%.

3.2. Liquid-air energy storage

LAES is a promising and novel long-term energy storage technology, suitable for mid- to large-scale applications. The technology employs liquid air or liquid nitrogen as the main working fluid and storage medium, providing a reasonably high volumetric energy density (50–80 kWh m^{-3}; see table 5 and note in section 4.1) compared to many of the other large-scale energy storage systems, and also with virtually no geographical constrains and environmental risks [6]. The LAES technology relies on well-established off-shelf components, minimising possible development risks and ensuring a long life span of 30–40 years [64]. It has a great flexibility under different off-design operation conditions and cross-sector integration with process industry, for example, for efficient waste heat/cold utilisation, and hence increasing the overall system efficiency [65]. In addition, considering a start-up time within a few minutes [66], a power rating of tens to hundreds of MWs and a discharge duration of several hours [64], LAES has a high potential for a variety of applications including energy management. One of the most interesting features of LAES technology is that it can simultaneously produce both electricity and cooling energy during the liquid air regasification/expansion process, respectively, where cold energy can be regarded as a free by-product [67]. From this perspective, LAES is being configured as a technological bridge between both the necessities to enhance RES exploitation and the cold-economy concept [68, 69]. Indeed, dealing with the compelling necessity to face the booming of cooling demand that may put at stake the reliability of the electricity grid, LAES is playing a crucial role as it has the potential to simultaneously provide electricity and cooling energy, above of all, during peak energy demand periods.

From the technical point of view, recalling the battery analogy as depicted in figure 9, a typical LAES system operation can be divided into three phases: charging, storage and discharging. During the charging phase, which often occurs when there is excess electricity at off-peak hours, electrical work is used to clean, compress and liquefy the air. Then, the liquid air is stored at a low pressure in insulated tanks. During the

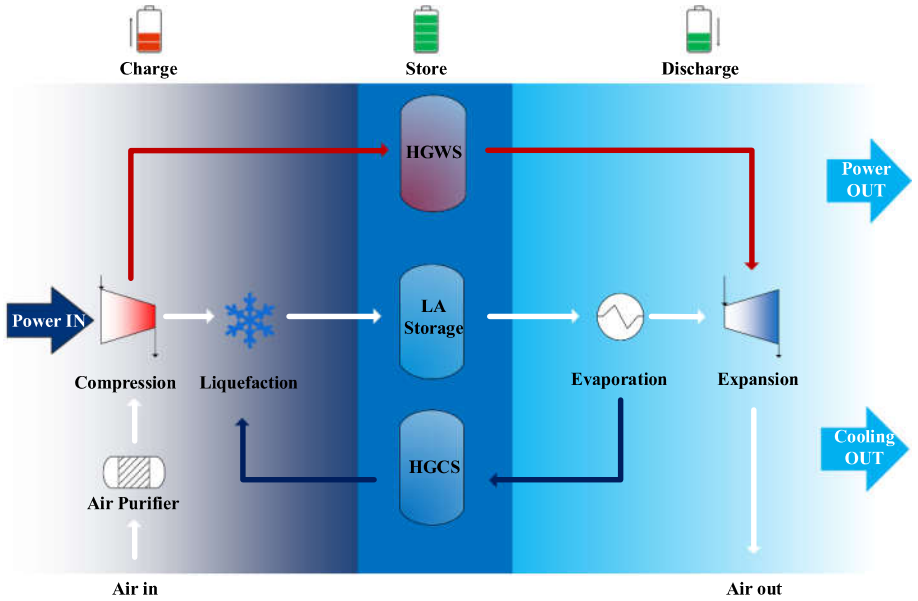

Figure 9. Schematic of a LAES system involving the processes of: (a) compression and liquefaction of air; (b) liquid air storage; and (c) regasification and expansion of air. The use of HGWS and HGCS can increase the round-trip efficiency.

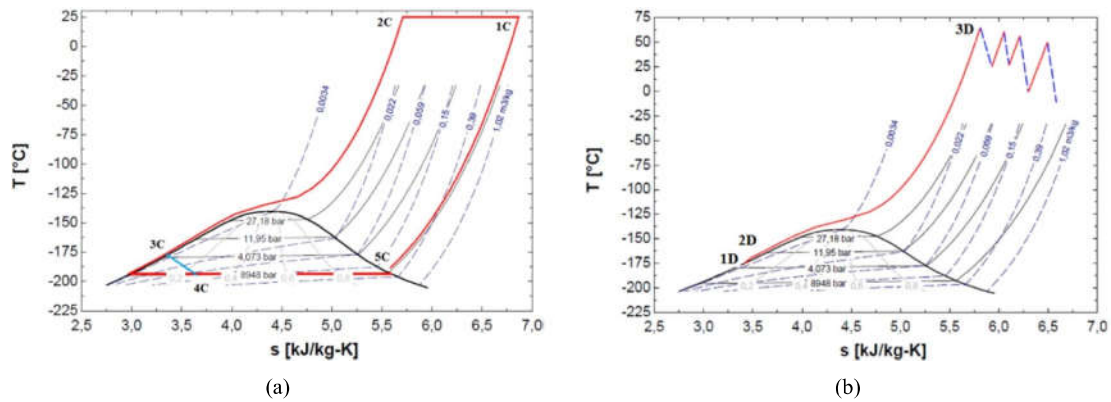

Figure 10. *T–s* diagram of the ideal LAES cycle for: (a) charging; and (b) discharging from [70].

discharging phase, when electricity demand is high, the liquid air is drawn from the storage tanks, pumped by cryogenic pumps, regasified to close to ambient temperature (or even higher if waste heat is available) and expanded in power-producing expanders such as turbines and piston engines to generate electrical work.

A potential way to increase the round-trip efficiency of LAES systems is via the implementation of warm and/or cold TES, namely a HGWS and/or a HGCS, respectively. As shown in figure 9, the main purpose of the two configurations is achieved by means of thermal coupling, where waste heat and/or waste cold phases (charging and discharging) operate asynchronously at different periods of the day. The thermodynamic cycle of the ideal LAES charging and discharging processes is demonstrated with a representative *T–s* diagram in figure 10, which is taken from the work of Sciacovelli *et al* [70].

The LAES concept was first proposed, independently, by Shepherd [71] in 1974 and Smith [72] in 1977 who introduced a thermodynamic cycle for air liquefaction, based on adiabatic compression and expansion turbomachinery. Another LAES concept was proposed by Mitsubishi [73] in 1997 and focuses on the LAES discharge section, in particular on the design of the cryogenic pump and the power turbine. Chino *et al* [74] studied a method to increase the LAES efficiency proposing a system that uses the liquid air produced with off-peak power at night time to feed a combustor of a gas turbine during day time. The whole LAES system was practically demonstrated by Highview Enterprises Ltd, now re-branded as Highview Power [75], leading to the world first pilot plant (350 kW_e/2.5 MWh) [76] (figure 11) and the first grid scale pre-commercial demonstration plant (5 MW_e/15 MWh) [77] (figure 12) based on the patent developed in collaboration with Chen *et al* [78] in 2007. The LAES systems are based on a Claude cycle, integrating a low-pressure cold TES,

(a) (b)

Figure 11. (a) External; and (b) internal views of the 350 kW_e/2.5 MWh LAES pilot plant [75].

Figure 12. External view of the LAES grid-scale demonstrator plant in Greater Manchester.

which can have a round-trip efficiency up to ∼60%. In both cases, external waste heat sources were used, namely a waste heat stream (up to 60 °C) released by a SSE (Scottish & Southern Energy) biomass power plant located in Greater London and engine exhaust gases from a Viridor landfill gas generation plant installed in Greater Manchester, respectively. In 2019, Highview Power has announced plans to construct the UK's first (50 MW_e/250 MWh) and the US's first (50 MW_e/250 MWh) commercial LAES-CRYOBatteriesTM, which will be located at a decommissioned thermal power station in northern England [79] and in northern Vermont (USA) [80], respectively.

A process flow diagram of the pilot plant is shown in figure 13. The first prototype comprised only a liquid nitrogen tank and a turbine, able to process 47% of the low-grade waste heat from a biomass plant. The liquefaction plant, based on Claude cycle and operating at a peak pressure of 12 bar with a liquid-air production rate of around 1.4 ton h^{-1}, was later commissioned and supplied by Chengdu Air Separation Corp., realizing the first LAES prototype in the world. The liquefaction cycle performance is enhanced by the sub-TES (HGCS) that recovers the high-grade waste cold energy discharged by the liquid-air regasification process. The waste cold is stored in a series of eight packed-gravel beds filled with quartzite rocks inside a container insulated with perlite. During discharging, liquid air is pumped at a peak pressure of 56 bar by means of two reciprocating cryogenic pumps and then regasified in two evaporators from the exhaust gases coming from the last turbine. The energy recovery cycle is based on an expansion train of four radial inlet turbines, with the air reheated after each single expansion by a water-glycol heat transfer fluid thermally coupled with the externally available heat source.

A summary of the LAES state-of-the-art is provided by categorizing studies in the literature according to their focus on: (a) standalone; (b) polygeneration; or (c) integrated/hybrid configurations, all discussed below and presented in table 2.

3.2.1. Standalone LAES system

A standalone LAES configuration refers to a system configuration not integrated with any external thermodynamic cycle and/or heat source/cold sink. The only energy input to the system is the electricity required to produce liquid air. In particular, integrating the advantages of both A-CAES and LAES, a standalone configuration includes:

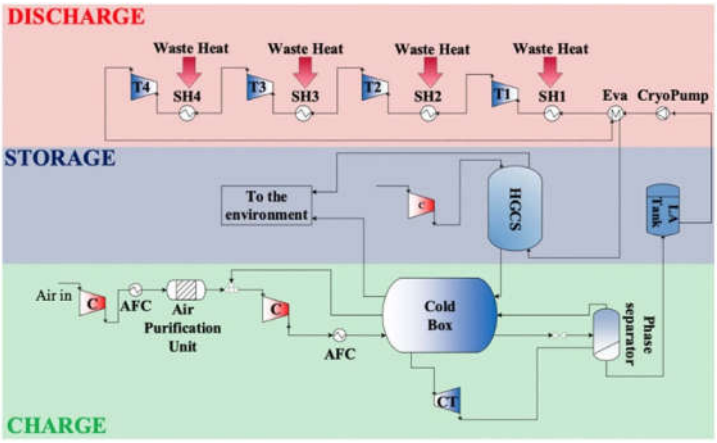

Figure 13. Process flow diagram of LAES pilot plant. Reprinted from [76], Copyright (2015), with permission from Elsevier.

Table 2. Main literature studies on LAES categorized by configuration type. Key performance indicators (KPIs) involve the round-trip efficiency η_{RT} and thermal efficiency η_{TH}.

Reference	Configuration type	Liquefaction cycle	Energy recovery cycle	HGCS configuration	KPI_{max}
Ameel *et al* [81]	Standalone	Linde–Hampson	Direct expansion	—	$\eta_{RT} = 43\%$
Guizzi *et al* [82]	Standalone	Claude	Direct expansion	Two tanks	$\eta_{RT} = 5\%$
Xue *et al* [83]	Standalone	Linde–Hampson	Direct expansion	Packed bed	$\eta_{RT} = 49\%$
Sciacovelli *et al* [84]	Standalone	Claude	Direct expansion	Packed bed	$\eta_{RT} = 50\%$
Hao Peng *et al* [85]	Standalone	Claude	Direct expansion	Two tanks	$\eta_{RT} = 62\%$
Chen *et al* [86]	Standalone	Linde–Hampson	Direct expansion	Packed bed	$\eta_{RT} = 67\%$
Comodi *et al* [87]	Polygeneration	—	—	—	$\eta_{RT} = 60\%$
Ahmad *et al* [88]	Polygeneration	—	Direct expansion, Brayton, Rankine	—	$\eta_{TH} = 74\%$
Al-Zareer *et al* [89]	Hybrid/ polygeneration	Claude	Rankine with fuel combustion	—	$\eta_{TH} = 72\%$
Tafone *et al* [67]	Polygeneration	Kapitza	Direct expansion	Packed bed	$\eta_{RT} = 45\%$
She *et al* [90]	Hybrid	Linde–Hampson	Direct expansion with ORC	Two tanks	$\eta_{RT} = 56\%$
Tafone *et al* [91, 92]	Hybrid/ polygeneration	Kapitza	Direct expansion with ORC and/or absorption chiller	Packed bed	$\eta_{RT} = 53\%$
Peng *et al* [93]	Hybrid	Linde–Hampson	Direct expansion with ORC and/or absorption chiller	Two tanks	$\eta_{RT} = 63\%$
Kantharaj *et al* [94]	Hybrid	Linde–Hampson	Direct expan- sion coupled with CAES	—	$\eta_{RT} = 53\%$
Farres-Antunez *et al* [95]	Hybrid	Linde–Hampson	Direct expansion coupled with PTES	—	$\eta_{RT} = 71\%$

- a charging phase, based on a recuperative thermodynamic cycle (Linde–Hampson [81, 83, 85] or modified Claude [82, 84, 91]);
- a discharging phase, based on direct expansion [84, 91], an indirect Rankine [96] or indirect Brayton [97] cycle, or a combination of the above methods;
- a storage section, either with an ambient pressure or pressurized liquid air tank [98];
- HGCS and HGWS systems, used to thermally couple the charging and discharging phases. For both TES systems, two different configurations have been proposed: packed-bed [84] and two-tank configuration [85, 93].

The standalone LAES system proposed by Chen *et al* [86] and Guo *et al* [99] denominated as SC-CAES, has been experimentally demonstrated with the first 1.5 MW SC-CAES pilot plant built by the Institute of Engineering Thermophysics (CAS) in Langfang, Hebei province of China [100] (figure 14). As of 2017 [101],

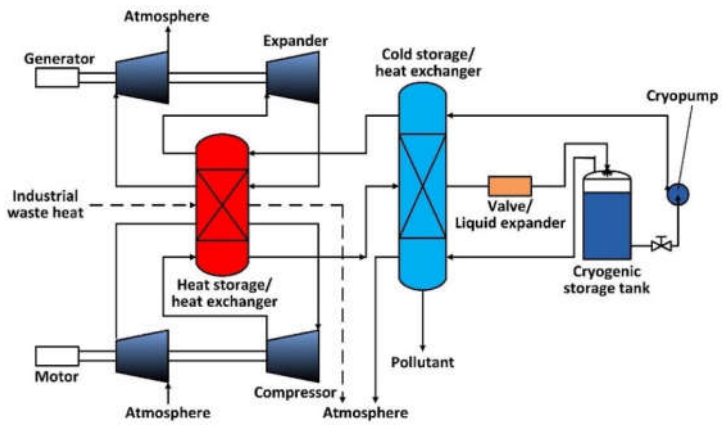

Figure 14. Schematic illustration of SC-CAES system. Reprinted from [88], Copyright (2016), with permission from Elsevier.

the SC-CAES system had successfully ran for more than 3000 h, achieving a system round-trip efficiency of about 55%.

3.2.2. Polygeneration LAES system

In order to extract most of energy stored in the form of liquid air, LAES has been designed as a polygeneration system providing cooling/heating and electrical power. The cooling load can be either provided directly by the cold energy released during liquid air regasification [87] or by the direct expansion of the gaseous air, imposing a constraint at the turbine inlet temperature [67]. The heating load potentially required for industrial uses and/or space heating/domestic hot water can be provided by the remaining waste heat discharged by the compression of air during charging [92]. Alternatively, the waste heat can be further exploited to run an absorption chiller to provide the required cooling load.

3.2.3. Integrated/hybrid LAES system

LAES hybridization has been proposed by many authors in different configurations and concepts, aiming to improve the thermal performance of LAES. Indeed, one of the main advantages of LAES system is represented by its thermo-mechanical nature that makes the energy storage capable to be integrated with other thermal energy systems, making efficient use of the available heat sources/heat sinks. Although other waste-heat recovery systems have been proposed, such as absorption chillers [89, 102] and Kalina cycle systems [103], ORC systems have been identified as the best solution to effectively utilize the waste heat released during charging, increasing LAES round-trip efficiency by up to 20% [90, 92] and decreasing the associated levelized cost of storage by up to 10% [91] (figure 15). Furthermore, Cetin *et al* [104] proposed a geothermal flash plant, in which, during peak times, additional heat is added from the geothermal resource to generate electricity. Hybrid systems combining LAES with other TMES systems, such as CAES [94, 105] and PTES [95], have been proposed in literature and found to improve the round-trip efficiency of the respective standalone systems by up to 10%.

3.3. Pumped-thermal electricity storage

PTES technology involves storing electricity in the form of heat, which can be either sensible or latent. PTES systems can be separated in three main categories: (a) Joule–Brayton PTES systems, which operate on similar principles to reversible Joule–Brayton[10] cycles; (b) transcritical PTES systems, which most often use CO_2 as the working fluid; and (c) CHEST systems, which are based on conventional steam Rankine cycle or lower-temperature variants employing organic working fluids. This section presents an overview of the operating principles and recent development of the three PTES types.

3.3.1. Joule–Brayton PTES systems

Several PTES concepts have been developed using an ideal gas as the power cycle working fluid. An exemplary schematic along with a representative *T–s* diagram of such concepts are shown in figure 16. During charging the working fluid is first compressed to high temperatures (1 → 2, see figure 16(b)). Heat is then transferred out of the cycle into the hot store (2 → 3) before being expanded to low temperatures

[10] These cycles are referred to as Joule cycles or Brayton cycles by different communities, so the term Joule–Brayton is used here for clarity.

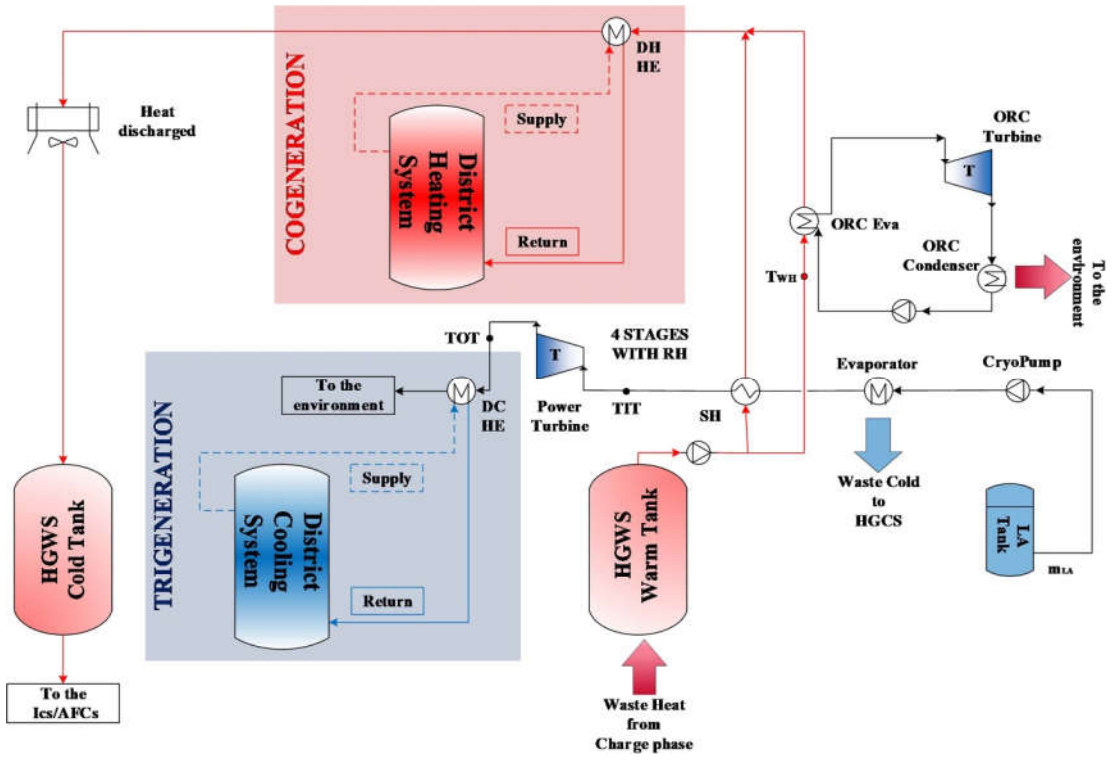

Figure 15. Integrated LAES and ORC system. Reprinted from [92], Copyright (2018), with permission from Elsevier.

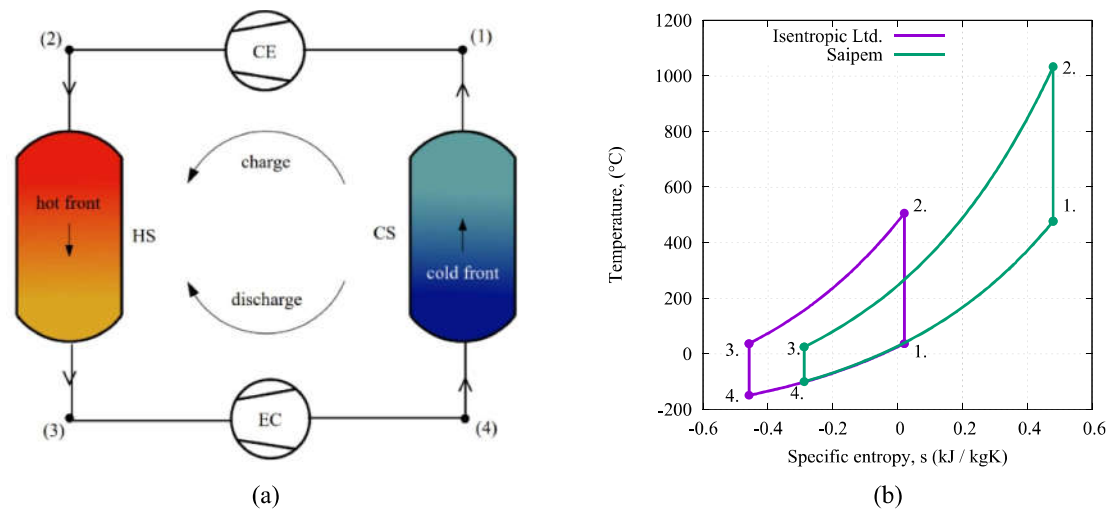

Figure 16. PTES system using solid thermal storage (thermoclines) such as the systems developed by SAIPEM and Isentropic Ltd: (a) schematic from [106]; and (b) T–s diagram of ideal PTES cycles using an ideal gas [106].

(3 → 4). Heat is subsequently transferred into the cycle (4 → 1) thereby charging the cold store. The discharging process reverses these steps so that electricity is generated from a Joule–Brayton heat engine which uses the hot store as the heat source and the cold store as the heat sink.

Most concepts use a closed cycle although an open cycle using air as the working fluid was proposed in 1979 by Weissenbach of MBB [107]. In that concept, air is compressed to 800 °C–900 °C and the heat stored in ceramic balls contained in steel tubes. Two concepts were subsequently invented simultaneously and independently in 2008–2009 and use argon in a closed cycle. SAIPEM proposed using maximum temperatures between 1000 °C and 1500 °C and storing the thermal energy in bricks of a refractory material such as clay with a high alumina or magnesia content [108]. Axial turbomachinery was used for the compression and expansion meaning that the system required four machines in total. Isentropic Ltd developed a cycle with lower maximum temperatures (∼500 °C) and used packed beds of pebbles as the

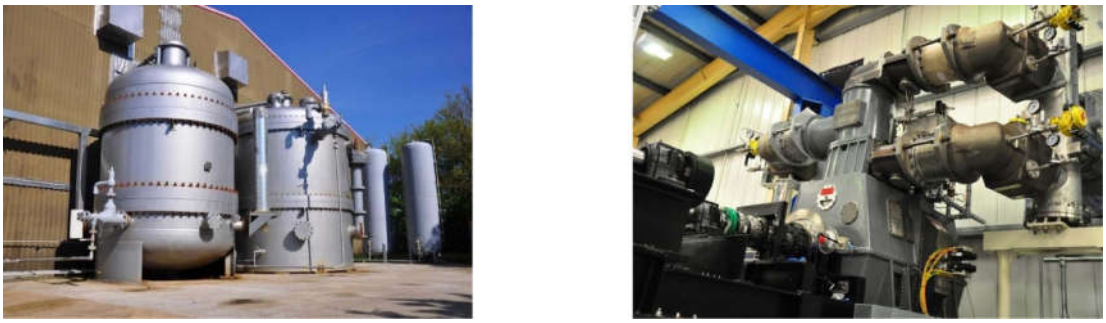

(a) (b)

Figure 17. Views of the: (a) packed-bed thermal stores; and (b) reversible reciprocating compression/expansion machine of the PTES system demonstrator developed by Isentropic Ltd and completed by Newcastle University [109].

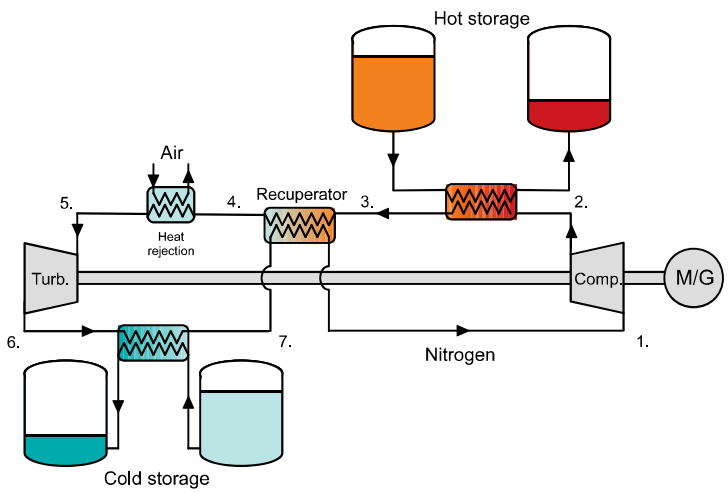

Figure 18. Schematic of a recuperated Joule–Brayton cycle with liquid stores as being developed by Malta Inc.

storage system [110] (figure 17). The packed beds could be 'segmented' to improve performance and flexibility. Isentropic Ltd also developed positive-displacement (in fact, reciprocating) engines that could be operated as both a compressor and an expander. Most recently, a Google X spin-out company known as Malta Inc. began development of a regenerated closed cycle [111, 112], as illustrated in figure 18. Malta Inc. aim to use commercial or near-to-commercial technologies for each component [113]. Thus, air-based turbomachinery is used for the compression and expansion, and temperatures are kept below 600 °C to reduce steel costs. Molten salts are used for the hot storage, while the cold storage uses a coolant such as glycol or isopropane.

Simple models of PTES systems can be developed analytically for Joule–Brayton cycles with ideal gases, and several expressions have been developed (see, for example [114–118], which use methods from first principles, endo-reversible thermodynamics, or classic cycle analysis). These expressions typically reveal the importance of certain parameters on the round-trip efficiency, which is particularly sensitive to the isentropic (or polytropic) efficiency of the compression and expansion machinery. Another important parameter is the work ratio, which is the ratio between the compression and expansion work during charging, with larger values improving the round-trip efficiency [114]. Similarly, the heat-to-work ratio provides an assessment of the total heat processed by the cycle for a given net work input. Large heat-to-work ratios are undesirable because, for a given net work input, a large quantity of heat must be transferred. Thus, heat transfer irreversibilities have a large impact on the cycle performance. Previous work has demonstrated that increasing the temperature ratio T_2/T_1 increases the work ratio and reduces the heat-to-work ratio (see figure 16 for numbering convention). On the other hand, increasing T_1/T_3 leads to higher work ratios, and therefore reduces the effect of compression and expansion losses, but the heat-to-work ratio increases, meaning that heat exchanger performance becomes more important, and that larger heat exchangers are required. The value of these parameters for several Joule–Brayton PTES systems is tabulated in table 3.

Table 3. Metrics for PTES variants described in the literature.

System		SAIPEM	Isentropic Ltd.	Isentropic Ltd.	Malta Inc.
Working fluid		Argon	Argon	Argon	Nitrogen
Storage type		Concrete	Packed bed	Packed bed	Liquid storage
Compression/expansion efficiency	%	90	90	99	90
T_2	°C	995	600	598	560
T_4	°C	−73	−164	−134	−59.9
$\beta = p_2/p_1$		4.6	10.9	7.6	4.6
$\tau = T_2/T_1$		1.69	2.83	2.23	1.58
$\theta = T_1/T_3$		2.52	1.00	1.26	1.70
Work ratio		5.29	2.84	2.81	3.17
Heat-to-work ratio		3.62	2.09	2.62	3.98
η_{RT}	%	67	59	87	59
Reference		[119]	[120]	[120]	—

These metrics can be used to inform the design of PTES systems by indicating which components are particularly influential on the cycle efficiency. As shown in table 3, Joule–Brayton PTES systems have comparatively low work ratios, and the design of efficient compressors and expanders is necessary to achieve reasonable round-trip efficiencies. The above trends may be generally applied to other PTES variants. For instance, systems that use sub-critical or transcritical cycles have much larger work ratios and are therefore less sensitive to compression and expansion losses. However, the phase changes that occur in these cycles also increase the heat-to-work ratio, which indicates that heat exchanger design is of primary importance.

The simplest implementation of a Joule–Brayton based PTES cycle was illustrated in figure 16, however different technologies and materials may be used at each stage of the process, so that a variety of concepts have been proposed. The rest of this section discusses trade-offs between Joule–Brayton PTES design decisions.

3.3.1.1. Open versus closed cycles

Power cycles can be either open or closed. Open-cycle systems draw (and release) air directly from the environment, thereby circumventing the need for (and costs associated with) heat rejection components and reducing capital/installation costs. Closed-cycle systems, on the other hand, require heat rejection components, but can be pressurized, which acts to increase the power density of the compression and expansion machinery, reduce the size of this machinery for a given power rating and, in theory, reduce the cost of these components. However, the cost of other components (such as heat exchangers, valves, seals) around the cycle can also be affected by higher pressures. A wide variety of working fluids may be used in a closed cycle, allowing the most suitable fluid to be used depending on the cycle configuration. For systems with direct thermal storage (i.e. thermocline systems), working fluids with a high ratio of specific heats ($\gamma = c_p/c_v$) are preferred from a thermodynamic perspective. These fluids go through a larger temperature ratio for a given pressure ratio ($\tau = \beta^{(\gamma-1)/\gamma}$), which reduces the costs of the storage pressure vessels [119, 121]. In this case, monatomic elements ($\gamma = 1.667$) such as argon are preferable to diatomic elements ($\gamma = 1.4$). On the other hand, cycles with indirect thermal storage do not require pressurized storage tanks. The system performance then depends on the heat exchanger performance. In [122], the heat transfer characteristics of several fluids were compared and it was found that elements with high c_p and low γ were preferable. The most promising fluids include hydrogen and helium, but their use is limited by cost, leakage and flammability issues. Furthermore, these fluids require many stages of compression or expansion in the turbomachinery. Argon has relatively poor heat transfer properties unless it is highly pressurized. Nitrogen may provide the best trade-off between performance, cost, and practicality, especially as existing air-based turbomachinery would require minimal or no modifications [115, 122].

A closed-cycle PTES cycle offers greater flexibility when choosing the temperatures at each point in the cycle. As mentioned above, the cycle analysis above indicates that it is preferable to increase T_1 above T_3 (figure 16(a)) as this leads to a higher work ratio. Such a cycle can enable a large temperature difference between the hot and cold stores with a lower pressure ratio, as indicated in table 3. As noted by [115, 122], systems with $T_1 > T_3$ have an 'overlap' in the heat transfer in the hot and cold stores. Heat can be exchanged between the high- and low-pressure sides of the cycle in a regenerator/recuperator to eliminate this overlap (figure 18), which reduces the total heat transfer area required. While the recuperation does not significantly affect the performance of the cycle, it allows the storage temperatures to be chosen more flexibly, which is particularly useful for liquid storage media which have more limited operational ranges than solids.

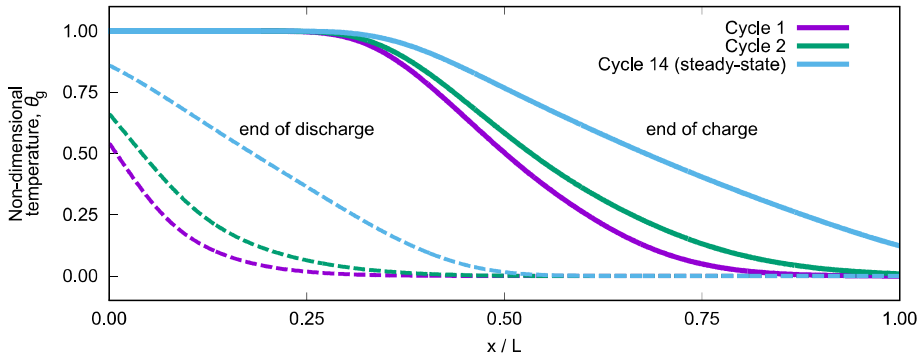

Figure 19. Thermal gradient (thermocline) along solid thermal store, in this case a packed bed. Reproduced from [123]. CC BY 4.0.

Part-load operation of closed cycles can be achieved using 'inventory control' [124] where the volume of working fluid in the cycle is adjusted. The pressure on the low-pressure side is adjusted proportionally, so that the volumetric flow through the turbomachinery remains constant. The machines can then be operated over the same pressure ratio, and therefore maintain the same temperature ratio. Not only does this mean that energy can be stored and extracted at the design temperatures, but the efficiency of each machine remains close to its design efficiency [125]. As a result, a closed-cycle Joule–Brayton PTES device can flexibly operate over a range of charging and discharging power ratings without affecting performance. Inventory control requires a buffer vessel of working fluid. The volume of this vessel may be minimized by locating it where the working fluid density is highest. Point 3 on figure 16(b) may be the most suitable location as it is close to ambient temperature which minimizes insulation requirements.

3.3.1.2. Thermal storage system

The most suitable materials to integrate with Joule–Brayton PTES cycles are sensible storage materials. The first Joule–Brayton cycles proposed using solid materials: Weisenbach's system used ceramic balls in steel tubes; SAIPEM's design used a concrete thermocline system; and Isentropic Ltd used packed beds of pebbles. Solid media can operate over a wide range of temperatures, have relatively high volumetric heat capacities, and are inexpensive and abundant. However, the power cycle fluid passes directly through these storage systems, requiring them to be pressurized and substantially increasing the cost. The thermal fluctuations also place additional stresses on the containment vessels (known as thermal ratcheting) which must be accounted for.

Solid storage systems are characterized by a thermocline, or thermal gradient, along the length of the store, as illustrated in figure 19. The thermocline presents several challenges to PTES design and operation. Firstly, the thermal gradient implies that it is not possible to fully charge the storage system without significant variations in the temperature of the exiting fluid [123, 126]. Thus, the storage system must be oversized in order to achieve the required storage capacity. Secondly, the variations in exit temperature may have implications for the rest of the cycle and must therefore be controlled appropriately [127]. These issues may be mitigated through various design modifications, such as the inclusion of electric heaters and heat rejection equipment [106], including PCMs at the ends of the store [128], or segmenting the thermoclines into several layers [129]. By carefully controlling which segments the working fluid travels through, segmented thermoclines can reduce pressure losses and temperature fluctuations [130], increase the energy capacity, and decrease stand-by losses [131]. Optimization studies found that PTES systems with segmented packed beds had slightly higher efficiencies (∼1%) and lower costs (∼10%) than non-segmented systems [106].

Using a liquid phase as the storage medium requires indirect heat transfer from the power cycle via a heat exchanger. Therefore, the liquid may not have to be pressurized (depending on its vapour pressure) which can reduce the cost of the storage tanks. These advantages were first described in [132] before being investigated in detail in [122, 133, 155], and explored for commercialization by Malta Inc. Liquids tend to have more limited operating temperature ranges and thus tend to be implemented in recuperated cycles. Liquids also have higher capital costs and may degrade over time. However, some relevant fluids—i.e. molten salts—have been widely deployed in CSP plants [134]. Thus, PTES can benefit from this operational experience and cost reductions. State-of-the-art nitrate molten salts are constrained to maximum temperatures below 565 °C due to degradation of the salt. However, recent developments in tank technology may allow the salt to be stable at temperatures up to 600 °C [135]. Temperature limits may be further

increased to over 700 °C by using chloride molten salts, although these salts are more corrosive, and higher temperatures may require the use of more expensive steels (if the tanks are not internally insulated) [134].

3.3.1.3. Compression and expansion machinery

Isentropic Ltd designed positive displacement machines which have the advantage that they can operate as both a compressor and an expander simply by changing the valve timing, thus reducing the number of machines from four to two. Isentropic Ltd made several developments to reduce pressure losses and heat transfer losses. However, minimizing losses leads to piston designs that have a large aspect ratio (bore-to-stroke length) [121]. As a result, custom-designed machines are required which leads to higher investment costs in the short-term while these technologies are commercialized. The heat transfer processes also require special consideration due to the thermal inertia of the cylinder walls [136, 137]. These machines are likely to be more suitable for smaller power ratings (<5 MW_e). However, a modular system could enable a device to achieve higher charging and discharging rates. Isentropic Ltd began the construction of these machines which was subsequently completed by Newcastle University, and these prototype devices reported achieve efficiencies in the range of 92%–94% [138].

Axial turbomachines are more cost-effective and efficient at larger power ratings (>50 MW_e), and therefore may be more suitable for larger-scale installations that are being developed in the near-term. Turbomachines for PTES systems may be quite similar to commercialized devices which therefore simplifies operation and maintenance issues as well as leveraging decades-worth of cost and performance optimization [115].

Conventional turbomachines run in one direction; i.e. they are either a compressor or an expander. While it may be theoretically possible to design a turbomachine that can run forwards (as a compressor) and backwards (and an expander), this will undoubtedly compromise the efficiency compared to two separate machines. However, reducing the number of machines from four to two could confer sufficient cost savings to make this approach worthy of further consideration.

3.3.1.4. Advanced Joule–Brayton PTES designs

The concepts developed by SAIPEM, Isentropic Ltd, and Malta Inc. provide an instructive introduction to PTES systems based on Joule–Brayton cycles. Several other systems have been proposed in the literature, which have either novel modifications or attempt to integrate PTES with other energy systems (see section 3.3.4).

Benato [139] added an electric heater to the charging phase of a Joule–Brayton PTES system with the aim of reducing the compressor pressure ratio, and therefore the cost. The electric heater increases the temperature of the air after the compressor, as shown in figure 20. The discharging cycle is the same as a conventional PTES cycle. This system achieved a round-trip efficiency of 9.5% at maximum storage temperatures of 1050 °C. This low value is partly due to the heater reducing the heat pump coefficient of performance, and partly because the thermal stores are 'unbalanced'; the heater increases the energy stored in the hot store without any increase in the energy stored in the cold store. As a result, the cold store discharges more quickly than the hot store, and not all of the hot energy can be extracted from the cycle (normally, the energy capacities of the hot and cold stores are linked by virtue of the heat pump). A similar system was proposed by Chen *et al* [140], who aimed to extract this excess heat using an additional engine during discharge. Incorporating an ORC system was found to improve the round-trip efficiency to 47.7%, which similar (although slightly lower) than a PTES system operating at lower temperatures without the electric heater (47.9%).

Robinson [141, 142] developed a PTES cycle with the aim of using 'ultra-high' temperatures to maximize the round-trip efficiency and energy density. In this system, energy is stored in molten aluminium between 1500 °C and 900 °C and is used to power a gas turbine. Robinson describes a containment vessel that reduces heat leakage losses through a combination of expensive metals (platinum and gold) and vacuums. Despite the complexity of the design, the author estimated the capital cost to be competitive with other large-scale electricity storage schemes.

Much of the literature on Joule–Brayton PTES cycles has considered the use of ideal gases, although real gases, such as sCO_2 may also be used [113]. sCO_2 has several advantages: for instance, its high density leads to compact turbomachinery which may lead to reduced costs. By operating close to the critical point, these cycles also achieve high work ratios (5–10) compared to ideal gas systems, due to the low expansion work during charging. However, heat-to-work ratios are also increased (∼9) so that the efficiency is quite sensitive to heat exchanger performance. The round-trip efficiencies of sCO_2–PTES cycles were found to be similar to ideal-gas PTES cycles. sCO_2 cycles face additional complexities due to the high operating pressures, and the large variation in CO_2 density near the critical point complicates part-load operation.

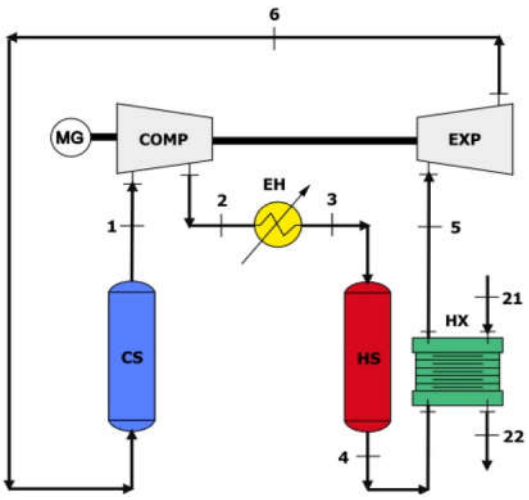

Figure 20. Schematic of a PTES charging phase with additional heat input from an electric heater. Reprinted from [139], Copyright (2017), with permission from Elsevier.

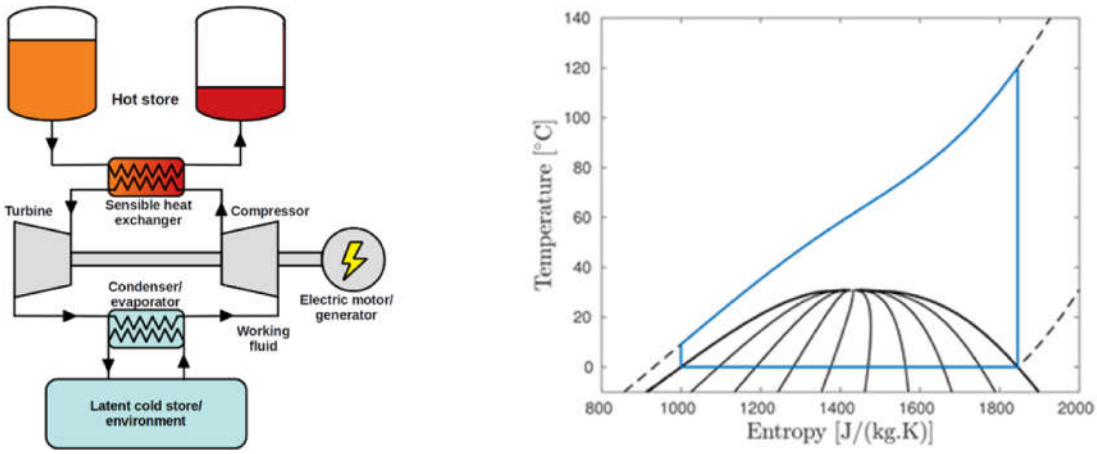

(a) (b)

Figure 21. (a) Plant layout; and (b) *T–s* diagram (right) of an ideal transcritical CO_2 cycle.

3.3.2. Transcritical PTES systems

Research on PTES systems based on transcritical cycles has predominantly taken place in Switzerland with input from the company ABB. Mercangöz *et al* [143] described a transcritical CO_2 cycle which used water as the hot storage and ice slurry as the cold storage. Most of the subsequent research has developed this type of cycle. Transcritical cycles resemble the Rankine cycle in that they have a condensation phase at the low-pressure side, but, because they reach supercritical conditions, they do not display a phase change at the high-pressure side. This means that thermal energy is exchanged fully in the form of sensible heat at the high-pressure side, similarly to Joule–Brayton systems.

A *T–s* diagram of an ideal, transcritical CO_2 cycle is shown in figure 21. The cycle operates over a smaller temperature range than Joule–Brayton cycles, with typical top temperatures in the range 95 °C–150 °C and bottom temperatures in the range −25 °C to 25 °C. This implies comparatively low energy densities and a high impact of heat-transfer losses on the round-trip efficiency, but also means that inexpensive storage materials can be used. Liquid water is well suited for the hot storage tanks, which may be pressurized or not, depending on the top temperature. The environment may be employed as source/sink to drive the evaporation/condensation phases, but Mercangöz *et al* [143] suggest the use of a salt-water/ice slurry as cold storage. This has the effect of lowering the bottom temperature and improving the work ratio of the cycle.

A general disadvantage of transcritical cycles is that the working fluid experiences strong specific heat capacity variations along the high pressure (supercritical) isobar. In order to minimize temperature differences (and their associated irreversibilities) along the heat exchange process, it is paramount to match

the heat capacity rates ($\dot{m}c_p$) of the working fluid and the storage fluid. Since the specific heat capacity of water is nearly constant, Mercangöz and subsequent researchers split the heat exchange process in a number of sections of varying water mass flow rate. This requires several hot water tanks operating at intermediate temperatures over different temperature ranges but enables a close agreement between the heat capacity rate of the CO_2 stream and the water streams at each section.

Matching the CO_2 saturation temperature and the ice slurry phase-change temperature requires the CO_2 to be at high pressure: around 30 bar on the low-pressure side and 140 bar on the high-pressure side. The high pressures add to the cost of pipes, valves and heat exchangers, but also mean more compact (and potentially cheaper) compressors and expanders. Compared to PTES systems employing direct heat exchange with packed beds, the cycle benefits from not needing to pressurize the thermal stores, unless water is used as storage medium at temperatures above 100 °C. If higher temperatures are desired but pressurization becomes too expensive, there is the possibility of using molten salts or heat transfer oils for the appropriate temperature ranges.

The use of liquid pumps or expanders means that transcritical systems can achieve higher work ratios than Joule–Brayton systems. Mercangöz *et al* [143] optimized a 50 MW transcritical CO_2 cycle and achieved a work ratio of roughly 6 and an efficiency of 65%. Morandin *et al* [144, 145] developed the work by Mercangöz *et al* [143] and described a modelling method based on pinch analysis. An optimization study gave an efficiency of 60% at a work ratio of 5. Morandin *et al* [146] also undertook a more detailed thermo-economic optimization of the system. The study optimized the system topology (i.e. the number of storage tanks and their layout). Morandin also investigated intercooling between the discharging expanders in this study.

Other studies done on the CO_2–PTES cycle include: (a) an analysis that proposes employing an isothermal compression/expansion stage and a regenerative process instead of the adiabatic compression/expansion stage, by Kim *et al* [116]; (b) a theoretical study (by Ayachi *et al* [147]) and an experimental study (by Tauveron *et al* [148]) of a system employing ground heat storage instead of hot water tanks; and (c) other parametric and control studies [149, 150].

Although system variants with CO_2 as the working fluid have received most of the research focus in the field of transcritical PTES systems so far, schemes based on other working fluids are also possible. In 2016, Abarr *et al* [151, 152] proposed a transcritical PTES system based on ammonia. The system operates at higher temperatures and is designed to be able to function either independently or as a bottoming cycle coupled to a gas peaking power plant. The authors suggest employing blocks of concrete (with an embedded heat exchanger) as thermal reservoir. The study displays an experimental analysis of the thermal stores. The experimental results are used to validate a numerical model of the plant, which predicts standalone storage efficiencies between 51% and 66% under varying levels of power rate and utilization of the stores.

More recently, Koen *et al* [153] presented a study where a wide range of working fluids were analysed as potential candidates for transcritical PTES cycles. In the study, over 150 working fluids are screened for thermodynamic, environmental and safety suitability. A resulting list of 8 'most suitable' fluids (which includes ammonia and CO_2) is then used by the authors to model the performance of a PTES system at a range of conditions and find optimum points. Three different storage materials (water and two types of thermal oil) were considered depending on the temperature range. A promising working fluid was found to be trifluoroiodomethane (R13I1), with a peak round-trip efficiency of 57%. The authors reckoned that these results could be further improved by employing multiple storage tanks (to reduce heat exchanger losses) and exploring different storage fluids, such as molten salts, which can operate at higher temperatures.

3.3.3. CHEST systems

A final category of PTES systems includes CHEST concepts, as illustrated in figure 22, which similarly to LAES have a relatively high volumetric energy density (40–100 kWh m^{-3}; see table 5 in section 4.1). CHEST concepts are based on conventional steam Rankine cycles, and do not feature cold storage. Low-temperature heat from the environment is used to generate saturated steam, which is compressed by electrical energy to enter the thermal store, where it is de-superheated, condensed and subcooled. A conventional Rankine cycle is then operated during discharging.

The first detailed suggestion made in 1920 [154] for the implementation of PTES was based on a combination of steam turbines and Ruths storage representing the state of the art at that time. Subcritical Rankine cycles using water as working fluid reach thermal efficiencies in the range of 30%–40% without requiring maximum process temperatures exceeding 400 °C, so the ratio between the heat stored and the mechanical energy released during discharging is in the range of 2–3. PTES based on steam cycles profits from the huge experience available for this technology from conventional power plants. In a typical configuration, the key parameters of the discharging cycle are similar to state-of-the-art Rankine cycles used in CSP plants or combined cycle plants. Isothermal heat transfer processes using wet steam as heat transfer

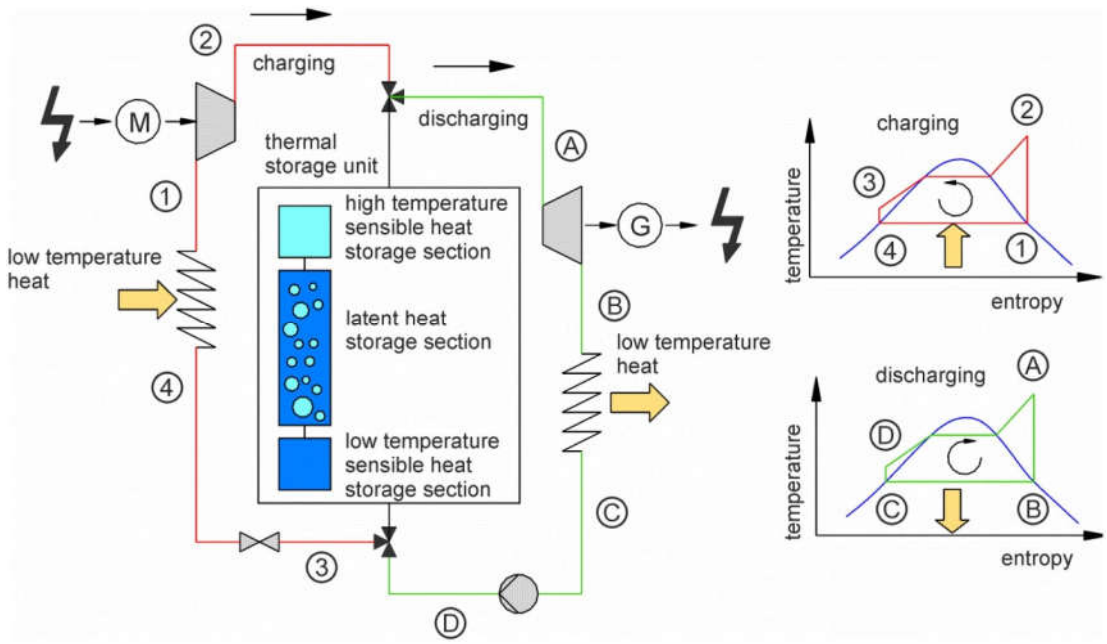

Figure 22. Schematic of the CHEST concept along with *T*–*s* diagrams of the charging and discharging cycles.

fluid are dominant in subcritical Rankine cycles, thus an efficient PTES implementation minimizing entropy generation demands an option for isothermal heat storage. The CHEST [155] concept foresees the combination of latent heat storage systems with steam compressors and steam turbines. This approach takes advantage of the progress made in recent years in the development of latent heat storage systems intended for solar-thermal power plants or industrial applications [156]. The CHEST concept uses water as the working fluid at a maximum pressure in the range of 100 bar for PTES systems intended primarily for the storage of electrical energy. While of-the-shelf components can be used for discharging and latent heat storage has reached an advanced state of maturity, new solutions have to be developed for steam compression in these pressure and temperature ranges. Compression technology can be evolved from turbines and modifications are required to meet efficiency targets.

A CHEST variant operated at lower maximum temperatures and pressures can also be implemented using an organic working fluid. The thermal efficiencies of ORC systems are lower, requiring larger heat storage capacities for a given capacity of mechanical energy, resulting in lower round-trip efficiencies for storage of electrical energy. The main components required for the implementation of a CHEST system using organic working fluids are in a more advanced state of maturity, with heat pumps reaching maximum temperatures of 160 °C being already commercially available [157]. At power levels up to 5 MW, systems using organic working fluids often have higher efficiencies than systems using water as the working fluid. ORC-CHEST is an interesting option for PTES systems intended for delivery of both thermal and electrical energy, where the lower round-trip efficiency is less relevant.

3.3.4. Integration of PTES systems with other energy sources and sinks

An advantageous feature of PTES arises from its ability to manage different energy vectors (electricity, heat or cold energy). During charging, PTES concepts behave in a similar manner to heat pumps: heat is transformed from a lower-temperature level to a higher temperature level. Charging might be not only needed to heat up the storage for later discharging, but might be also useful for cooling, e.g. in data centres or in manufacturing processes. If thermal energy at an elevated temperature from a waste-heat source is used to charge the storage system, the mechanical work needed in the charging process is reduced, thus improving the round-trip efficiency. If the lowest temperature during discharging is sufficiently below the temperature of the waste-heat source used during charging, the electrical energy delivered during discharging might even exceed the electrical energy used during charging. This is an interesting option for the utilization of low-temperature waste heat. During discharging, a PTES system might deliver both electrical energy and heat depending on the specific demand structure. If heat is also used, the requirements concerning the efficiency of components in a PTES system can be significantly reduced. There is also the option to adapt the ratio between delivered heat and delivered electrical energy according to the specific demand structure depending on seasonal variations. A first implementation of an experimental PTES system for management

of heat and electrical energy based on the CHEST concept is developed in the EC-funded CHESTER project [158], where a combination of heat pump, latent heat storage and expansion engine will be used for the storage and delivery of both heat and electricity.

Several systems that combine solar energy and PTES have been proposed. In one implementation a sub-ambient PTES system is supplemented by low-temperature heat from solar collectors [159]. The ammonia-based PTES device creates an ice-on-coils cold storage during charging and uses the environment as the hot storage. During discharging, heat is provided by the flat solar collectors, and is rejected into the cold store. Another concept uses separate heat pump and refrigeration systems for the hot and cold storage, respectively [160]. Both devices are charged by PV arrays, and solar thermal collectors are used to supply heat to the heat pump evaporator. PTES can also be integrated into higher temperature CSP systems. For instance, Farres-Antunez *et al* [161] suggested that a high-temperature heat pump using the Joule–Brayton cycle could be used to charge the molten-salt thermal stores at an existing CSP plant. Aga *et al* proposed a similar concept using a sCO_2-based heat pump [162]. Such systems would be able to top up the thermal stores when solar resource decreases—e.g. during the winter—and thereby increase the utilization of the power block. In a similar scheme [113], a heat pump was proposed as a means to increase the power output of a sCO_2 cycle at a CSP plant by over 10%, although the net generation of electricity decreased by a small quantity.

Several studies have investigated whether the flexibility of conventional thermal power plants can be improved by adding energy storage capabilities. For instance, Vinnemeier *et al* [163] considered the design of heat pumps that could create high-temperature thermal storage to be used in a steam cycle. Both transcritical and supercritical (i.e. ideal gas) heat pumps were considered, and it was found that, at high temperatures (up to 600 °C), it was preferable to use ideal gases. Heat pumps that were supplemented by an electric heater to reach higher temperatures were also considered, and it was found that although there is an efficiency penalty, such a system may simplify the heat pump design.

The transcritical PTES system described in the work of Abarr *et al* [151, 152] has several modes of operation depending on when it is preferable to generate power from natural gas, or store grid electricity and then later return it to the grid. The system can operate as a standalone PTES cycle where hot storage is created by the heat pump, while the environment is used as the cold storage. This heat can later be discharged through the ammonia heat engine. Alternatively, waste heat from the natural gas power plant can be used to charge the hot storage to about 400 °C–450 °C. The ammonia cycle may also act directly as the bottoming cycle to the natural gas plant, thereby generating power immediately rather than storing it for later use.

In another variation [164], it is proposed to give existing coal-fired power plants a 'second life' by converting these into electricity-storage devices. The plants are retrofitted with molten-salt thermal storage which may be charged by electric heaters or heat pumps, and the thermal energy can be dispatched through the existing power block. This system has the advantage of making use of existing equipment and infrastructure, although it is unclear how significant the modifications to the plants will be.

Other projects have investigated how PTES may be integrated with a variety of thermal systems. For instance, Frate *et al* [165] describe a system that uses low-grade waste heat as the cold source of the heat pump, thereby upgrading this heat to higher-temperature levels. The stored heat is discharged through an ORC system and a variety of fluids are considered. Jockenhofer *et al* [166] also describe how heat from various sources such as geothermal or solar thermal could be upgraded in a heat pump and stored. Waste heat from the discharging process could then be used to provide domestic heating. Several other studies have considered how PTES-like systems can be integrated into buildings in order to manage heating, cooling and electrical loads. For instance, Schimpf *et al* [167] describe a ground-source heat pump that stores thermal energy in a hot water tank. The tank may be supplemented by heat from a solar-thermal collector. Heating and hot water may then be provided to a building or converted back to electricity in an ORC system. Similar systems were also described in [168, 169]. These devices tend to have very low ORC system efficiencies, due to the small temperature range across the system. However, their flexibility provides value both in terms of electricity storage and heat and electricity production for buildings.

Farres-Antunez *et al* [95] proposed an advanced concept whereby a PTES topping cycle is integrated with a LAES bottoming cycle. By combining these cycles, the need for the cold liquid stores is removed, thereby reducing the required quantity of storage media and the cost per unit of energy capacity. Several configurations of the combined cycle were proposed, and they were found to have higher efficiencies and energy densities than either PTES or LAES. However, these advantages come with increased complexity and a higher cost per unit power [122], meaning that such combined cycles would be better suited to applications with medium/long charge/discharge duration times.

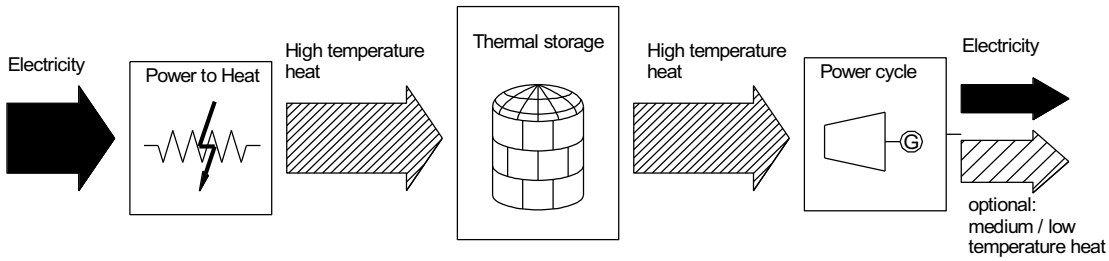

Figure 23. Basic principles of PHP storage systems.

3.4. Electrical heating and heat-to-power

Electrical heating and heat-to-power systems, also known as PHP systems, involve a straightforward concept: charging a thermal energy store using electrical heating and discharging using a thermal cycle [17]. The conversion of electricity into thermal energy causes exergetic losses; even in ideal systems, the maximum efficiency $\eta_{\mathrm{RT,max}}$ is limited by the maximum temperature T_{max} and minimum temperature T_{cold} in the PHP system according to Carnot:

$$\eta_{\mathrm{RT,max}} = \eta_{\mathrm{c,dis}} = 1 - \frac{T_{\mathrm{cold}}}{T_{\mathrm{max}}} \tag{3}$$

where $\eta_{\mathrm{c,dis}}$ is the discharge Carnot efficiency. In real systems, electricity is converted into heat at high first-law efficiency. The round-trip efficiency can be estimated by the efficiency of the thermal cycle used in the discharging process $\eta_{\mathrm{TH,dis}}$:

$$\eta_{\mathrm{RT}} \approx \eta_{\mathrm{TH,dis}}. \tag{4}$$

Figure 23 shows the basic principle of PHP. In the power-to-heat unit, the electrical energy is transformed into heat which is used to charge the thermal store. During discharging, the heat is converted back into electricity. If only electricity is delivered during discharging, a major share of the electricity used for charging is released as low-temperature waste heat. Due to the limited efficiency of pure electricity storage, CHP concepts may be considered, delivering also thermal energy for industrial processes or district heating during discharging.

The PHP concept requires an externally fired power cycle. Rankine cycles are a preferred solution for this, since compared to Brayton cycles they can reach similar thermal efficiencies at lower temperatures. Attonaty *et al* [170] presented a hybrid combined-cycle concept which uses fossil-fuel firing to increase the temperature of the air exiting the electrically charged thermal storage system. PHP based on Rankine cycles for discharging can profit from the experiences gained in CSP applications: a solar-tower system with an integrated two-tank molten-salt store can be transformed into a PHP plant by replacing the solar receiver by a component which heats the molten salt electrically; achieving estimated round-trip efficiencies in the range of 40% for systems exceeding a nominal power of 20 MWe. For smaller systems, alternative thermal storage concepts with reduced operational effort might be preferred:

- Systems using packed beds combined with closed-air cycles allow wider operational temperature ranges (from ambient up to 800 °C for hot stores) compared to molten salts (260 °C–560 °C). Besides the smaller footprint, the avoidance of freezing and reduced corrosion issues are also attractive advantages. Electrical heating of air is cost-effective and, in contrast to molten salts, local overheating of the heat transfer medium beyond permissible maximum temperatures is not critical.
- Latent heat storage allows the direct heating of the storage material, avoiding an intermediate fluid cycle during charging. By integrating electrical heating rods into the PCM volume, the ramp-up time during charging can be reduced significantly allowing the utilization of fluctuating energy sources. Since the exergetic efficiency of the charging process is not relevant in PHP concepts, large temperature differences are possible, avoiding the power density limitations typical in latent-heat storage systems. The storage capacity can be increased significantly by using the storage material in both the solid and liquid state. Latent heat storage system can be designed modular, allowing the adaptation to specific requirements. The minimum nominal power depends mainly on the available power cycle.

For systems below a few $\mathrm{MW_e}$, the employment of ORC systems may be preferred, especially at lower storage temperatures (<400 °C–500 °C), due to their suitability in these power and temperature range [171].

Table 4. Technical characteristics of TMES systems. Systems currently being envisioned by manufacturers or that are currently under development fall within these ranges.

Technology	Discharge power rating (MW)	Rated discharge duration (h)	Rated discharge energy capacity (MWh)	Charge power rating (MW)	Rated charge duration (h)	Round-trip efficiency (-)	Geographical constraint	Reference
Diabatic CAES	10–320	2–24	640–2640	50–60	8–40	54%–60%	Yes	
Adiabatic CAES	0.5–300	1–24+	1–1000	—	1–24+	60%−70%	Yes[a]	[21, 175–177]
Isothermal CAES	1.3–1.6	0.5	1	2.2	1	38%[b]	Yes[a]	
Standalone LAES	1–300	4–120	4–36 000	1–900	4–360	45%–70%	No	[6, 64, 76, 178]
Joule–Brayton cycle PTES	10–150	6–20	80–3000	10–150	6–72	50%–75%	No	[114, 115, 120]
CO_2 cycle PTES	10–100	2–5	20–500	10–100	3–10	48%–65%	No	[116–159]
CHEST	10–100	6–72	80–7200	10–150	6–72	60%–70%	No	[17, 115]

[a] An above-ground pressurized vessel can be used for small-scale systems (e.g. <10 MW). See also the analysis in figure 33 and related text in section 4.2.3.
[b] Goal 80%.

The application of direct energy conversion is an alternative approach for the implementation of PHP. In the work of Datas *et al* [172], an electrically charged high-temperature storage system is combined with a thermo PV generator. This concept requires no moving parts and is interesting for small systems delivering both heat and electricity.

All components required for the implementation of a PHP system are already commercially available. Regarding the round-trip efficiency, PHP approaches those of D-CAES systems, without being restricted by geological requirements.

4. Unified assessment and thermo-economic comparison

This section provides a unified assessment and thermo-economic comparison of TMES systems. First, the characteristics of the different systems are analysed and compared at their intended power rating and discharge duration in section 4.1. This analysis is based on technology configurations proposed by industry and literature, focusing on concepts intended primarily for electricity storage. Although advanced concepts based on polygeneration systems or systems integrated with additional heat sources have been discussed in section 3, these are often associated with different cost and performance characteristics. A comparison between polygeneration and only-electricity systems would require more complicated analysis [17] and is out of the scope of this section.

The cost and performance characteristics of TMES systems largely depend on the application and system size. In order to account for the effect of scale, a like-to-like comparison is presented in section 4.2 to examine the competitiveness of the possible options at varying discharge power rating and discharge duration. In this effort, thermo-economic models of the main TMES options are developed. It is vital that all technologies are assessed using a unified framework, which means that whenever different systems utilize similar components, the use of consistent cost correlations and performance metric assumptions is adopted. Lastly, section 4.3 discusses TMES systems as an alternative option to commercially available PHES and battery systems.

4.1. Thermo-economic comparison at discharge power ratings and discharge durations derived from literature

A comprehensive analysis of TMES systems has been conducted and the performance and cost characteristics are presented at their intended power ratings and discharge durations in tables 4 and 5. These are derived from both industrial applications (plants in operation, demonstration plants) and academic research. Figure 24 shows a comparison of discharge power rating and rated discharge duration of the different types of TMES options, indicating the ranges for which each system has been considered. For comparison purposes, PHES systems, VRB flow batteries and Li-ion batteries are also included [6, 11]. It is clear from figure 24 that TMES systems are intended to provide high power ratings.

Table 5. Additional technical characteristics along with TRLs of TMES systems. Systems currently being envisioned by manufacturers or that are currently under development fall within these ranges.

Technology	Energy density (kWh m^{-3})	Power density (kW m^{-3})	Power capital cost ($ kW^{-1})	Energy capital cost ($ kWh^{-1})	Maturity (TRL)	Operational lifetime/cycle life: Time (year)	Operational lifetime/cycle life: Cycles	Reference
Diabatic CAES	3–15	0.5–2	1050–1480	4–50	TRL 9	20–40	25 000	
Adiabatic CAES	0.5–20	0.5–2	970–1200	20–220	TRL 5–6	20–40	—	[7, 24, 37, 179–183]
Isothermal CAES	3–6	0.5–2	4980	—	TRL 5–7	—	—	
Standalone LAES[a]	50–80	0.5–17	900–6000	240–640	TRL 7[b]	30–40	10 000–15 000	[6, 64, 76, 178]
Joule-Brayton cycle PTES	20–50	1–15	1000–6000	100–500	TRL 2–5	30	—	[114–120]
CO_2 cycle PTES	10–15	2–7.5	500–2500	250–400	TRL 2–4	>25	—	[116–159]
CHEST	40–100	0.5–17	1500–6000	200–600	TRL 2[c]	30	10 000	[17, 155]

[a] LAES energy and power densities are calculated, as are those of all other listed technologies, by taking into account all system components, including both the volume of the liquid-air storage tank and the volumes of the sub-thermal energy stores (HGWS and HGCS). If only the volume of the main storage medium, namely liquid air, is considered in the definition of those KPIs, the range of energy and power densities are 120–200 kWh m^{-3} and 1–40 kW m^{-3}, respectively.
[b] Expected TRL 9 in 2021.
[c] Expected TRL 4 in 2021.

More specifically, all options in tables 4 and 5 except I-CAES, which still involves a large potential for development, target power ratings that can be higher than 10 MW and discharge durations that can be longer than 24 h. Some of the options target even higher power ratings: it has been already proven that D-CAES systems achieve power ratings higher than 300 MW (Huntorf plant), while A-CAES and LAES can also be designed at these sizes. The intended discharge power ratings of Joule–Brayton PTES, CO_2-based PTES and CHEST systems are similar (10–100 MW, 10–100 MW and 10–150 MW, respectively). In terms of discharge duration, LAES systems target applications ranging from 4 h to more than 5 d, while CHEST systems also target longer discharge durations (up to 3 d). CO_2-based PTES systems target lower discharge durations (<5 h) than PTES systems based on the Joule–Brayton cycle or the CHEST concept. At durations close to or higher than 24 h, technologies like Li-ion or lead-acid batteries cannot compete (they have nominal discharge durations lower than 10 h [6]), which is one of the main advantages of TMES systems.

The round-trip efficiency of the different TMES systems, as well as PHES systems, VRB flow batteries and Li-ion batteries is presented in figure 25. As shown, most TMES options show similar efficiency estimates, close to 60%. CAES has experienced huge advancements in the last decades, with round-trip efficiencies increasing by more than 20% [6, 7, 173], and although it is now considered a commercialized technology, there are prospects for significant efficiency improvements [174]. Standalone LAES systems have often showed relatively lower round-trip efficiencies in the past (e.g. 43% [81] or 49% [83]), however recent research shows increased performance (e.g. 62% [85]). Furthermore, various designs of PTES systems based on the Joule–Brayton cycle have been explored, showing that optimal designs of closed-cycle systems can achieve high efficiencies (∼65% [20]). Transcritical CO_2-based systems, which do not display a phase change at the high-pressure side, show similar efficiencies to Joule–Brayton systems (48%–65%). Furthermore, although CHEST concepts operate at lower maximum temperatures than Joule–Brayton PTES systems, they achieve similar round-trip efficiencies (65% [17]). In general, PHES systems show higher round-trip efficiencies than TMES systems (70%–87%), while VRB flow batteries and Li-ion batteries also show promising efficiencies (60%–90%) [6, 17]. However, although the efficiency of TMES systems is generally slightly lower than PHES and battery systems, the gap is not significant. TMES systems are at an earlier stage of development and projections demonstrate that the gap can get smaller in the very near future. In addition, the efficiency of TMES systems can be significantly improved when they take advantage of waste heat (e.g. more than 20% increase has been demonstrated for LAES [90, 92] and CHEST [17]), while these systems can be used for the delivery of both electricity and heat, which are not available options for PHES and battery systems.

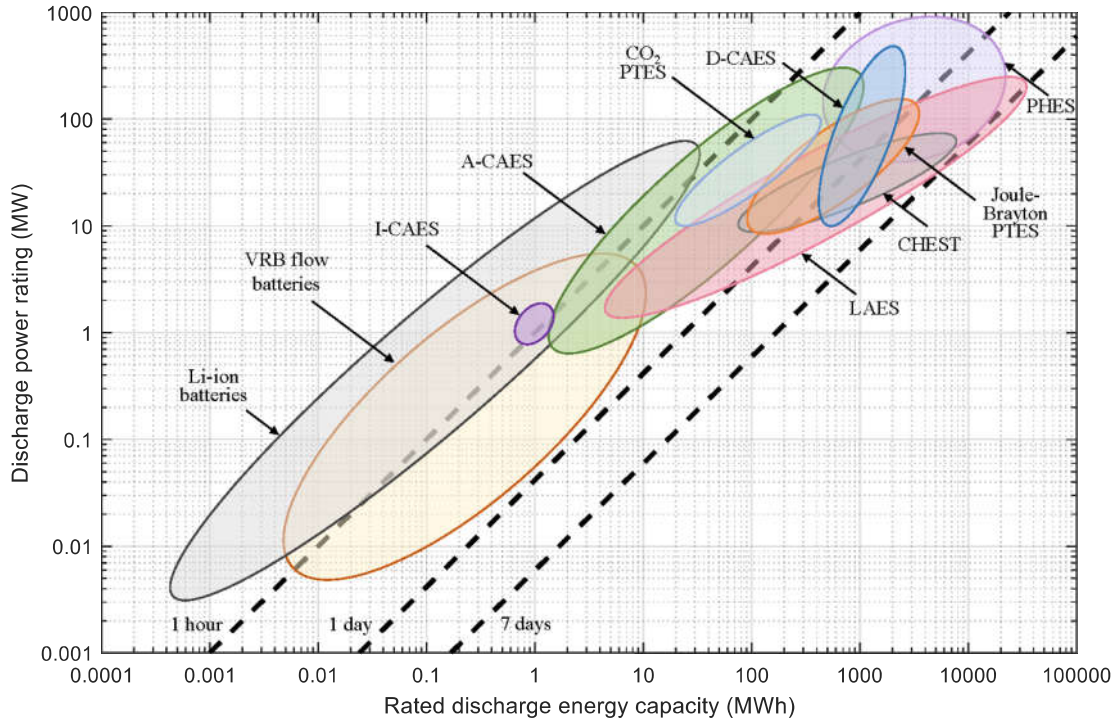

Figure 24. Discharge power rating and rated discharge energy capacity for TMES systems. The black diagonal lines represent discharge duration at the given discharge power rating and rated discharge energy capacity. PHES systems, VRB flow batteries and Li-ion batteries are included for comparison purposes.

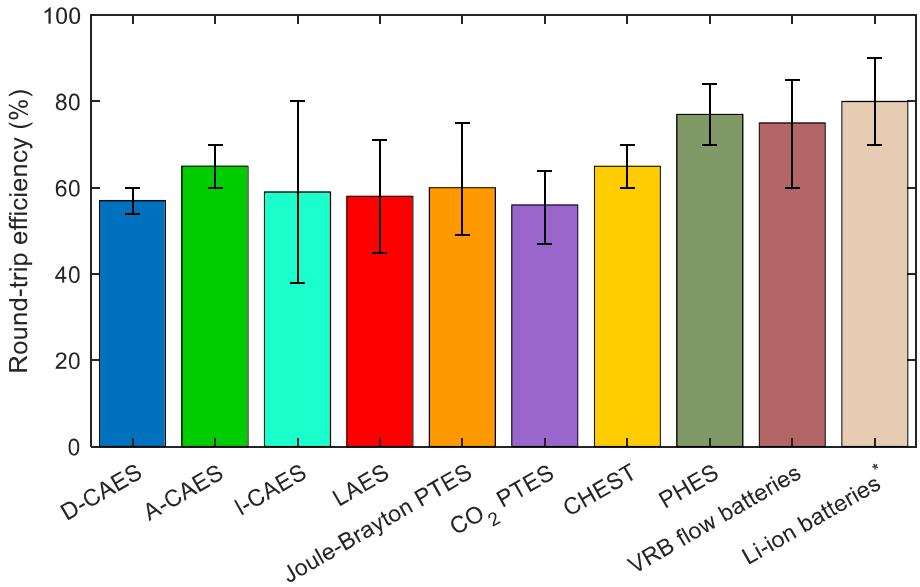

Figure 25. Round-trip efficiency of TMES systems (specifications in table 4). PHES systems, VRB flow batteries and Li-ion batteries are included for comparison purposes. Error bars signify the min-max ranges reported in literature. For a unified analysis based on a consistent performance and cost estimation methodology, please refer to section 4.2. * N.B.: Li-ion batteries are less suitable and not intended for long-duration (>10 h) or long-lifetime (>15 years) storage applications.

The power and energy densities of different TMES options are reported in figure 26, which again includes PHES and battery systems for comparison purposes [6, 13]. Figure 26 shows that LAES represents a very interesting solution in terms of both energy and power density. LAES systems experience energy densities in the range 50–80 kWh m^{-3}, which are about 3–25 times higher than CAES (3–15 kWh m^{-3}) and about 25–160 times higher than PHES (0.5–2 kWh m^{-3}). The high energy density is considered one of the biggest advantages of LAES, which, in standalone configurations, involves no geographical constraints either. The lower requirements for space mean 'ease' of storage and low environmental damage. Concepts based on

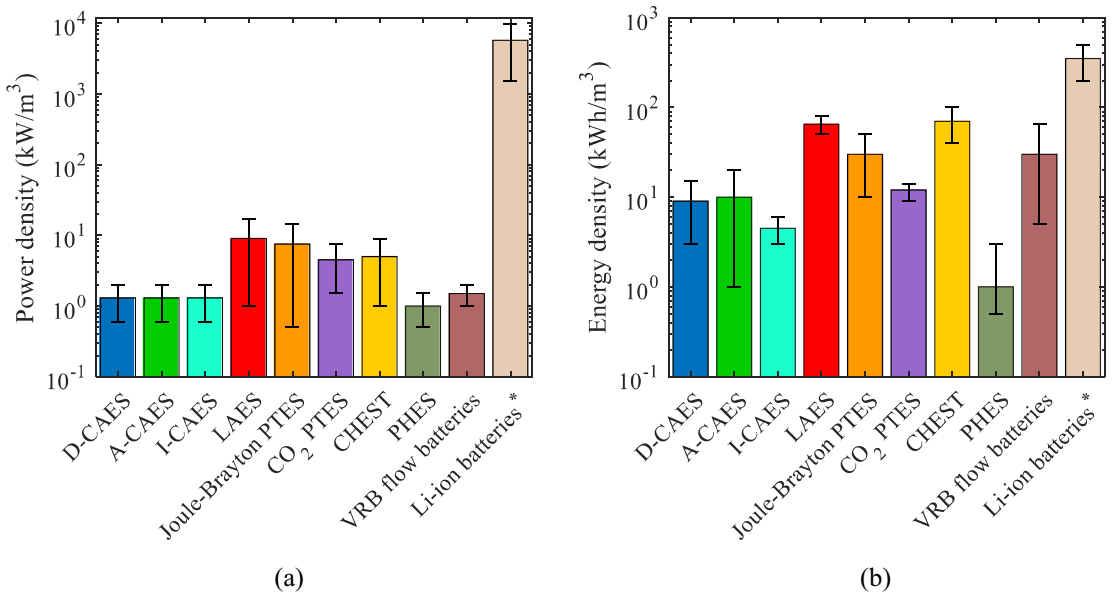

Figure 26. (a) Power density; and (b) energy density of TMES systems (specifications in table 4). PHES systems, VRB flow batteries and Li-ion batteries are included for comparison purposes. The plots are logarithmic on the ordinate and error bars signify the min-max ranges reported in literature. For a unified analysis based on a consistent performance and cost estimation methodology, please refer to section 4.2. * N.B.: Li-ion batteries are less suitable and not intended for long-duration (>10 h) or long-lifetime (>15 years) storage applications.

PTES also experience no geographical constraints and significantly higher energy and power densities than CAES and PHES systems. The CHEST concept, which involves no cold storage system, targets high energy densities in the range 40–100 kWh m^{-3}. When compared to TMES systems, flow batteries approach similar energy densities but have lower power densities. Li-ion batteries are dominating in terms of both power and energy density [6, 11], and are therefore a strong candidate for low-duration storage applications where space is important.

The maturity level of the different systems is measured by the TRL, which is a measure developed by NASA and often used by many authorities including the European Commission [184]. As shown in figure 27, D-CAES, PHES, VRB flow batteries and Li-ion batteries are deployed technologies that have reached a mature state, even though significant research on these concepts is still on-going. A-CAES and I-CAES are at an earlier stage of development and involve significant prospects to be further deployed in the next years. Furthermore, LAES has seen undergoing breakthroughs and is soon going to reach a TRL of 9 (2021), equal to D-CAES, PHES and flow batteries. Systems based on PTES are still in the development or research stage, and as they evolve, components can be modified to further reduce irreversibilities; therefore, these systems are expected to experience notable improvements in both performance and cost effectiveness. In this effort, the Annex 36 of the IEA's Technology Collaboration Programme kicked off in 2020 aiming to help the latter systems to market and provide basis for proper regulations [185].

TMES systems have life expectancies in the range of 20–40 years, which is a significant advantage when compared to any type of large-scale battery system (usual lifetime of 10–15 years [6]). PHES systems, on the other hand, have the longest life expectancy which is close to 60 years [17]. In addition, depending on the investment in insulation, the self-discharge of TMES systems can be low (<1%), which is an important advantage for long storage-duration applications when compared to conventional batteries [6].

It is worth mentioning that batteries in general involve significant embedded energy, i.e. energy required for manufacture. A measure referred to energy stored on invested (ESOI) is often used to compare grid-scale electricity storage options in this regard [186]. The ESOI is defined as the ratio of energy stored over the lifetime of a technology over the embodied primary energy. The comparison of ESOIs of different storage options in the work of Barnhart *et al* [186] reveals that storage methods based on thermo-mechanical concepts have a performance that can be an order of magnitude higher than competing electrochemical options (a value of 240 is reported for CAES compared to a value of 2–10 for various battery technologies).

TMES systems are analysed and compared to PHES, VRB flow batteries and Li-ion batteries in terms of power capital cost (cost over discharge power rating) and energy capital cost (cost over rated discharge energy capacity) as derived from industrial applications and academic research in figure 28. Five main conclusions

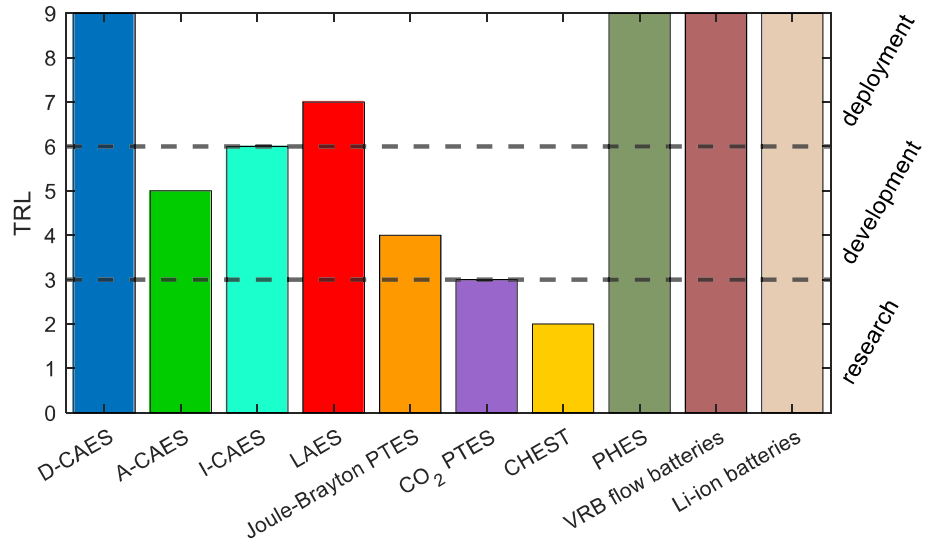

Figure 27. Level of maturity (TRL) of TMES systems (specifications in table 4). PHES systems, VRB flow batteries and Li-ion batteries are included for comparison purposes.

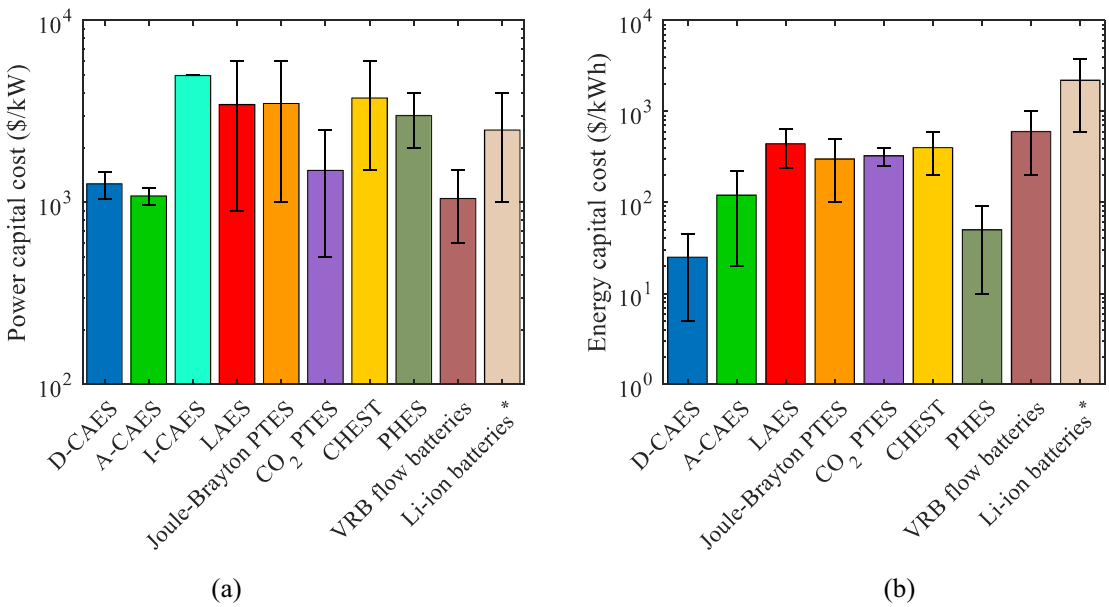

Figure 28. (a) Power capital cost; and (b) energy capital cost of TMES systems (specifications in table 4). PHES systems, VRB flow batteries and Li-ion batteries are included for comparison purposes. The plots are logarithmic on the ordinate and error bars signify the min-max ranges reported in literature. For a unified analysis based on a consistent performance and cost estimation methodology, please refer to section 4.2. * N.B.: Li-ion batteries are less suitable and not intended for long-duration (>10 h) or long-lifetime (>15 years) storage applications.

can be drawn: (a) D-CAES and PHES, which are commercially available and mature technologies for larger-scale electricity storage, are associated with the lowest energy capital cost (<50 \$ kWh^{-1}); (b) CO_2-based PTES systems shows promising power capital costs, even though they are associated with a low TRL of 2–4; (c) VRB flow batteries and Li-ion batteries experience significant energy capital costs compared to TMES systems (~600 \$ kWh^{-1} and ~2000 \$ kWh^{-1}, respectively); (d) both the power and energy capital cost of LAES, Joule–Brayton PTES and CHEST systems are very close to each other (~3500 \$ kW^{-1} and ~400 \$ kWh^{-1}, respectively); and (e) the uncertainty in the cost of LAES and PTES systems is significant (±3000 \$ kW^{-1}, ±200 \$ kWh^{-1}), since these technologies are still developing and costs significantly depend on the intended discharge power rating and discharge duration of the system. Furthermore, it is worth highlighting that as these costs correspond to technologies intended for different discharge durations, a direct comparison of these values can be misleading, e.g. PHES is generally intended for medium/long-duration storage and therefore appears significantly cheaper. A complete economic

analysis of TMES systems and their comparison to other types of storage requires a comparison at equal capacities, which involves considering how component costs change at different scales. This analysis is conducted in section 4.2.

4.2. Thermo-economic comparison as a function of power ratings and discharge durations

The thermodynamic principles described in section 3 are used to develop simple thermodynamic models of the main TMES options (CAES, LAES, Joule–Brayton PTES and CHEST systems), aiming to capture how their characteristics vary at different scales. In order to provide a like-to-like comparison between the systems, it is assumed that all air-based turbomachines have a state-of-the-art isentropic efficiency of ∼90%. Similarly, heat exchangers are designed for an effectiveness (ratio of actual to maximum possible heat transfer) of ∼95%. Since the isentropic efficiency of turbomachinery and heat exchanger effectiveness in this analysis are kept constant, the round-trip efficiency and energy density of the systems do not vary with discharge power rating or duration. Therefore, this section focuses on the variations of power capital cost, energy capital cost and power density.

4.2.1. Thermodynamic model description

4.2.1.1. LTA-CAES model

LTA-CAES overcomes the challenges of high-temperature compression and high-temperature TES of A-CAES, achieving higher round-trip efficiencies. For this reason, a LTA-CAES model is developed, similar to the one in figure 6, section 3.1.2. Two separate configurations are considered: (a) one that assumes that an air-tight chamber (e.g. salt cavern) is available; and (b) one that involves compressed air being stored in high-pressure, carbon-steel storage vessels with added costs, but without the geographical constraints associated with the former configuration. The systems in both cases involve a four-stage compression process, a four-stage expansion process and eight heat exchangers (each compression/expansion stage is followed by heat exchange). Heat is stored in the form of pressurized water (150 °C). The air-storage pressure varies between 4 and 10 MPa.

4.2.1.2. LAES model

The developed LAES model involves a standalone configuration, with no integration of any external thermodynamic cycle or source/sink. The process flow diagram, similar to the one shown in figure 13, section 3.2, includes the three characteristic phases: charging, storage and discharging. The charging phase allows to turn the gaseous air at ambient pressure and temperature into liquid air by means of the Kapitza thermodynamic process which includes two-stage intercooled compression, and the liquid air is then stored in a low-pressure cryogenic tank. During the discharging phase, the liquid air is pumped to high pressure and evaporated: the excess cold released during the evaporation process is stored in a cold thermal energy store (HGCS). The high-pressure gaseous air is then reheated in 4 stages at the end of which it is expanded through a turbine producing electricity. The heat of compression stored in a hot thermal energy store (HGWS) is used to further increase the air temperature at the inlet of each superheater. The heat transfer fluids employed in the HGWS and the HGCS are Therminol 66 and air, respectively.

4.2.1.3. Joule–Brayton PTES model

The most developed PTES concepts are based on the Joule–Brayton cycle. These systems can involve different thermal storage options. Two separate models are considered here. The first is based on a liquid-tank thermal storage system and is designed to roughly correspond to the PTES concept being developed by Malta Inc. (section 3.3.1). In this system, molten salt and a water-glycol mixture are used for the hot and cold TES materials, respectively, while the working fluid is nitrogen. To match these storage fluids, the maximum temperature is 560 °C and the minimum temperature is −28 °C. The maximum pressure ratio is ∼3 and the maximum pressure is ∼3 MPa.

The second model roughly corresponds to the PTES concept developed by Isentropic Ltd (section 3.3.1), which involves packed beds of pebbles (magnetite, Fe_3O_4) for the TES material and argon for the working fluid. Design guidelines from [106] were used to inform the geometry and operation of the packed-bed stores. The packed-bed model follows the methodology set out in [106, 130], although storage losses have been neglected to be consistent with the other modelling results used in this article. The hot packed bed is a pressure vessel that operates at a pressure of ∼1 MPa and the cold packed bed is not pressurized. Both tanks are internally insulated to reduce the temperature that the steel containment is exposed to.

4.2.1.4. CHEST model

A CHEST system intended primarily for delivery of electric energy during discharging is based on a steam cycle with a maximum pressure in the order of 10 MPa not exceeding a temperature of 360 °C. Analyses have

shown that higher-temperature steam results only in minor improvements which do not justify the higher costs. This pressure level is chosen as it allows the application of $NaNO_3$ as latent-heat storage material. Latent-heat storage systems using $NaNO_3$ have been demonstrated in larger-scale (in the order of MW) systems. State-of-the-art latent heat storage systems are based on a regenerator concept using a heat exchanger embedded into the storage material. The design includes two molten-salt tanks added to the PCM storage for preheating and superheating. The PCM storage is considered active; which is an advanced concept based on the transport of the storage material through a heat transfer section. In this concept, the mass of storage material is chosen independently from the discharge power of the system. Active-PCM concepts have been demonstrated in lab-scale storage systems. Active PCM reduces the complexity of the thermal storage system used in the CHEST concept. Especially for long discharge durations, the advanced PCM concept is expected to reduce costs.

4.2.2. Economic/costing methodology

Cost data for most of the TMES systems are not available, so estimations are conducted based on past literature data and cost surveys. The main components of each system are costed individually and then added to provide the total cost estimate. All cost estimates are converted to the appropriate currency assuming currency rates for conversion from GBP (£) to USD ($) and from EUR (€) to USD ($) to be 1.17 $/£ and 1.08 $/€. The costs are also adjusted for inflation and other economic conditions by using:

$$C_a = C_b \left(\frac{I_a}{I_b}\right) \tag{5}$$

where C_b and C_a are the costs at data collection time and analysis time, respectively, and I_b and I_a are the cost indexes at base and present year, respectively. Cost indexes used are based on the chemical engineering plant cost index [187].

The substantial uncertainties involved in costing have been discussed in the work of Georgiou *et al* [18], which utilizes mean estimates from a variety of costing methods. In this review paper, a similar approach is used. The main idea is to estimate all component costs (compressors, expanders, heat exchangers, storage tanks, motor/generators) using three main correlation methods (Turton *et al* [188], Seider *et al* [189] and Couper *et al* [190]) and acquire mean estimates, which are then added up to provide system cost estimates. In all the mentioned studies, the base cost of each component $C^0{}_B$ is estimated in USD ($) using:

$$\log\left(C_B^0\right) = K_1 + K_2 \log(A) + K_3 [\log(A)]^2 \tag{6}$$

where A is the capacity or size of the component being investigated and K_1, K_2 and K_3 are parameters specific to that component.

Depending on the type of each component, this cost is multiplied by additional factors associated with installation and commissioning, the material selected, the selected design and pressure at which the component operates (for pressurized storage vessels). The units of A, the value of the parameters K_1, K_2 and K_3 and the additional factors vary between the three methods. Also, the cost correlations provided can only be used for certain ranges: above a certain size, they cannot be considered reliable. In order to overcome this problem, it is assumed that when larger components than those for which correlations can predict costs are required, multiple units of the same components are installed in parallel. In the case of larger-scale compressors and expanders ($\geqslant$50 MW), due to the inadequacy of the above methods to provide reliable estimates as these are outside of the ranges for which the correlations were generated, a compressor cost correlation from Valero *et al* [191] is used instead.

The cavern storage costs for the LTA-CAES system assume a solution-mined salt cavern and are estimated using [192, 193], which include the costs of drilling, development, dewatering and piping. For the LTA-CAES system configuration that includes compressed-air storage vessels, it is assumed that the largest possible vessel size is 1000 m^3, which is at the upper limit of our presently available correlations for pressure vessels, and that in the need for larger volumes, vessels of this size are installed in parallel. In the case of the liquid-tank PTES system, molten salt and glycol are assumed to have a cost of 1 $ kg^{-1} . For the packed-bed Joule–Brayton PTES system, magnetite is associated with a cost of 0.139 $ kg^{-1} [18] and the insulation cost is 1500 $ m^{-3} . The latter system also requires an electric heater to manage the temperature variation at the exit of the cold store, which is costed as indicated in [139]. In the case of CHEST, costing information has been obtained directly from industrial partners.

4.2.3. Thermo-economic performance maps

4.2.3.1. Power and energy capital costs

The thermo-economic analysis of the developed LTA-CAES, standalone LAES, Joule–Brayton PTES and CHEST system models is presented in figures 29–32. For all technologies, as the rated discharge power rating

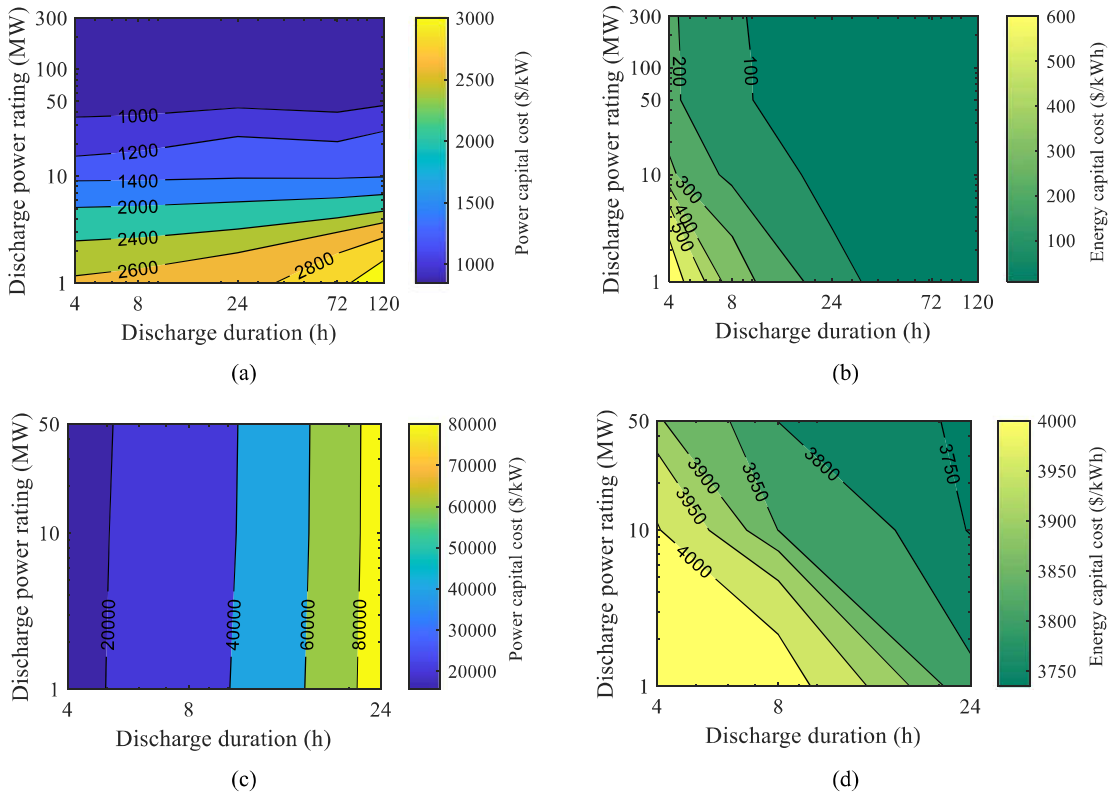

Figure 29. Thermo-economic analysis of a LTA-CAES system for varying discharge power rating and discharge duration: (a) power capital cost assuming underground salt cavern is available; (b) energy capital cost assuming underground salt cavern is available; (c) power capital cost assuming compressed air is stored in carbon-steel pressure vessels; and (d) energy capital cost assuming compressed air is stored in carbon-steel pressure vessels. The system operates in the pressure range of 4–10 MPa and involves a four-stage compression and a four-stage expansion process. The TES material is pressurized water. The plots are logarithmic on both axes.

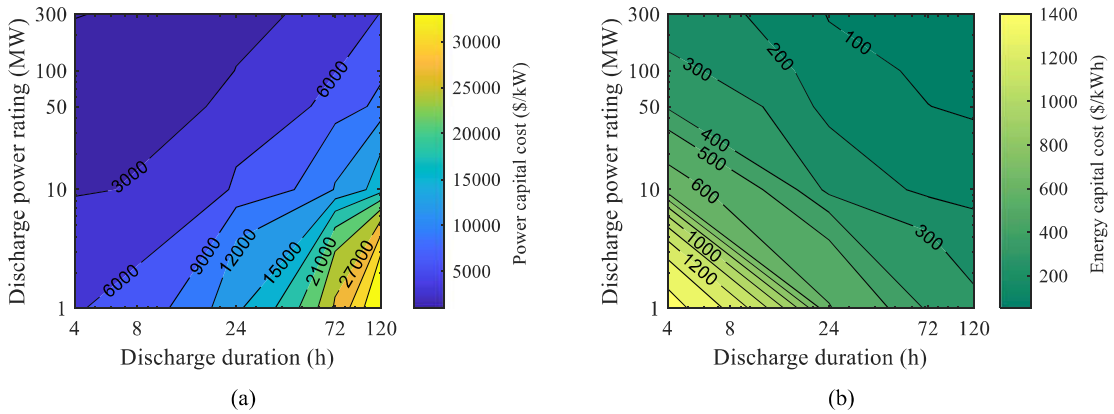

Figure 30. Thermo-economic analysis of a standalone LAES system for varying discharge power rating and discharge duration: (a) power capital cost; and (b) energy capital cost. Gaseous air is turned into liquid air using two-stage intercooled compression. During discharging, the liquid air is pumped to high pressure, evaporated, and then the high-pressure gaseous air is reheated in four stages and expanded through a turbine. The model includes warm and cold TES (HGWS and HGCS) and the heat transfer fluids employed in the HGWS and the HGCS are Therminol 66 and air, respectively. The plots are logarithmic on both axes.

increases, the power and energy capital costs reduce significantly. As the discharge duration increases, on the other hand, the impact on the power and energy capital costs is different: (a) the power capital cost increases since the same power is provided using a larger store; and (b) the energy capital cost reduces, as any costs associated with power-related technologies (compressors/expanders) remain constant.

When an underground salt cavern is available, the LTA-CAES system is associated with the lowest cost at all considered sizes. For power ratings above about 40 MW, the power capital cost of the LTA-CAES system reduces below 1000 \$ kW^{-1} (figure 29(a)). For longer discharge durations (>24 h), the energy capital cost (figure 29(b)) drops to low values (<100 \$ kWh^{-1}). When the power rating is high (>50 MW), these low

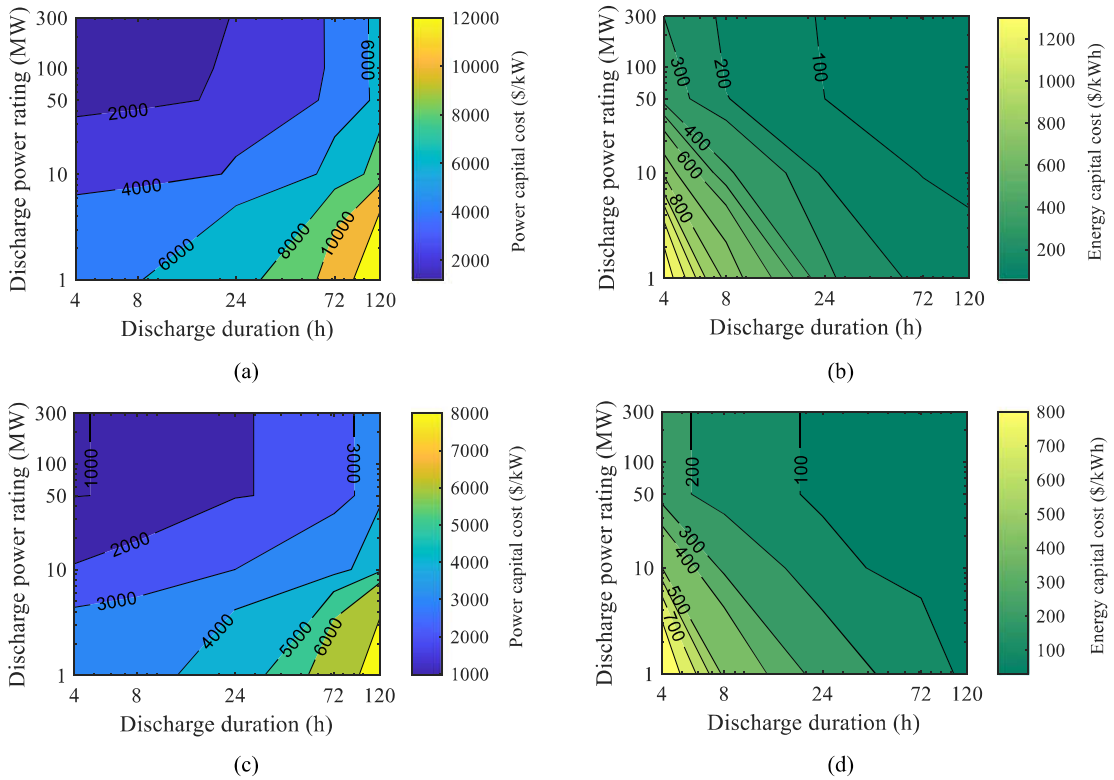

Figure 31. Thermo-economic analysis of two PTES systems based on the Joule–Brayton cycle for varying discharge power rating and discharge duration: (a) power capital cost for a system with liquid-tank TES; (b) energy capital cost for a system with liquid-tank TES; (c) power capital cost for a system with packed-bed TES; and (d) energy capital cost for a system with packed-bed TES. The liquid-tank system operates in a pressure range of ∼0.3–3 MPa, uses nitrogen as working fluid and uses molten salt and water-glycol mixture as hot and cold TES materials, respectively. The packed-bed system involves a pressure vessel operating at 1 MPa and uses magnetite and argon as TES material and working fluid, respectively. The plots are logarithmic on both axes.

costs are achieved even at short durations (∼10 h). Although the costs of caverns are low, the installation of such systems is constrained to locations where suitable geographical features are available. Since the energy that can be stored depends on the availability of these features but is not associated with significant additional costs, the power capital cost (figure 29(a)) increases only slightly with discharge duration. The cost of small-scale CAES systems is also relatively low; the energy capital cost of a 1 MW, 4 h system is about 600 $ kWh^{-1}, which is significantly lower than other options at this scale.

CAES systems could, instead of utilizing existing air-tight chambers, employ high-pressure compressed-air vessels, which would make the systems independent of the availability of geographical features and therefore the chosen location. However, such vessels have not yet being widely exploited at large scale, due to the large volumes and high pressures involved, and the very high costs of materials and installation. The power and energy capital costs of CAES systems based on pressure vessels are shown to be very high (figures 29(c) and (d)). These costs include an allowance for associated platforms and ladders [189]. Since the highest share of costs of these systems is attributed to the vessels and therefore to the amount of energy stored, the power capital cost (figure 29(c)) is shown to mainly depend on the discharge duration. The energy capital cost remains very high (∼3800 $ kWh^{-1}) even for power ratings and discharge durations higher than 10 MW and 8 h, respectively. One of the reasons for this is that the maximum size of a single tank considered in this analysis is 1000 m^3, and it is likely that, if significantly larger storage vessels are built in the future, they will benefit from further economies of scale that can bring down the costs presented here.

The standalone LAES does not depend on geographical location, which is made possible by the fact that the air is in liquid form and it can be therefore stored in a much smaller and lower-pressure tank than what would be required for CAES. This store, however, is associated with a notable cost, something which is clear in figure 30(a): the power capital cost increases significantly with discharge duration. Especially for high-duration (>24 h), low-power (<10 MW) applications, the power capital cost of LAES becomes very high (>15 000 $ kW^{-1}). The high energy density of LAES translates to a promising energy capital cost ((figure 30(b)), which drops below 200 $ kWh^{-1} for systems with power ratings and discharge durations higher than 10 MW and 12 h, respectively, and even lower (<100 $ kWh^{-1}) for systems with power ratings and discharge durations higher than 50 MW and 24 h, respectively.

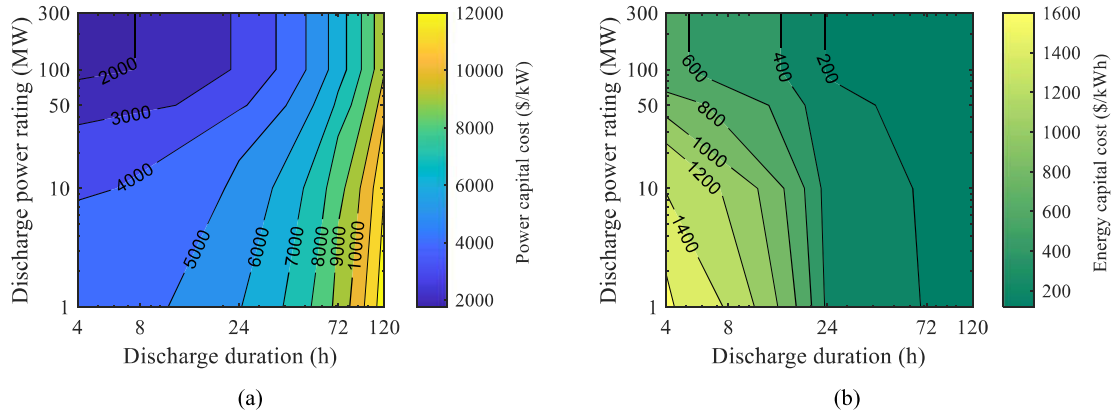

Figure 32. Thermo-economic analysis of a CHEST system for varying discharge power rating and discharge duration: (a) power capital cost; and (b) energy capital cost. The system is based on a steam cycle with a maximum pressure of ∼10 MPa and a maximum temperature of 360 °C. $NaNO_3$ is used as the latent-heat storage material. Active PCM storage is considered. Two molten-salt tanks are added to the PCM storage for preheating and superheating. The plots are logarithmic on both axes.

Designs of Joule–Brayton PTES systems based on a liquid-tank and packed-bed thermal storage solutions have notable differences, therefore cost variations with discharge power rating and discharge duration are analysed for both types of systems (figure 31). In terms of power capital cost (figures 31(a) and (c)), both configurations are shown to be more expensive than CAES but cheaper than LAES systems, especially at longer discharge durations. PTES systems that use either liquid-tank thermal storage or packed-bed thermal storage can both achieve very similar round-trip efficiencies in the region of 60%, however the configuration based on packed-bed TES shows more promising power capital costs, achieving values lower than 2000 $ kW^{-1} for discharge power ratings and discharge durations higher than 50 MW and lower than 24 h, respectively. At low power ratings (∼1 MW) and discharge durations (∼4 h), the energy capital costs of both the liquid-tank and packed-bed configurations are lower than those of LAES, with the packed-bed system being again favourable (1200 $ kWh^{-1} and 800 $ kWh^{-1}, respectively). This is primarily because the liquid-tank system uses four tanks and effectively the equivalent volume of two tanks is always empty when fluid is moved from one tank to another. Using a single-tank thermocline could increase the energy density but would be associated with high mixing losses. As a result, PTES systems based on packed beds have higher power and energy densities and therefore achieve lower costs per unit energy and power compared to systems that use liquid tanks. However, it is likely that in practice, systems with large energy capacities are more likely to use two-tank liquid storage. This is due to the physical size constraints of packed-bed pressure vessels being lower than the size limits of liquid-storage vessels. While a packed-bed system could achieve high energy capacities by placing many packed beds in parallel, this system would be more complicated to engineer than a system with large liquid tanks. Several concepts are being investigated where two-tank systems can be substituted by a single liquid tank containing a hot and a liquid region, therefore reducing empty tank space and cost, although they are yet to be commercialized [194].

The CHEST concept shows relatively higher power and energy capital costs than the Joule–Brayton PTES configurations, even though the difference is not large. The power capital cost (figure 32(a)) ranges from less than 2000 $ kW^{-1} for high-power, low-duration systems to about 12 000 $ kW^{-1} for low-power, high-duration systems. At low power ratings (∼1 MW) and discharge durations (∼4 h), the energy capital cost is close to 1600 $ kWh^{-1} (figure 32(b)), while when the discharge duration raises above 24 h, the energy capital cost falls below 400 $ kWh^{-1}, no matter the discharge power rating.

The power and energy capital costs of all investigated systems are directly compared at three different discharge power ratings (1 MW, 10 MW, 300 MW) and varying discharge duration (1–120 h) in figure 33. Four main observations can be made from this figure: (a) when an air-tight chamber is available, the LTA-CAES system is predicted to have the lowest power and energy capital costs at all sizes; however, (b) when pressure vessels are used for the storage of compressed air in LTA-CAES, the power and energy capital costs are very high and, therefore, these systems show low competitiveness; (c) the power and energy capital costs of the LAES system are high at small discharge power ratings (1 MW), but the LAES system becomes competitive as the discharge power rating increases (>10 MW), such that this technology shows particular promise for large-scale storage applications; (d) Joule–Brayton PTES systems based on packed-beds show promising power and energy capital costs, and as the rated discharge duration increases (>24 h), they show lower costs than the other non-geographically-constrained options.

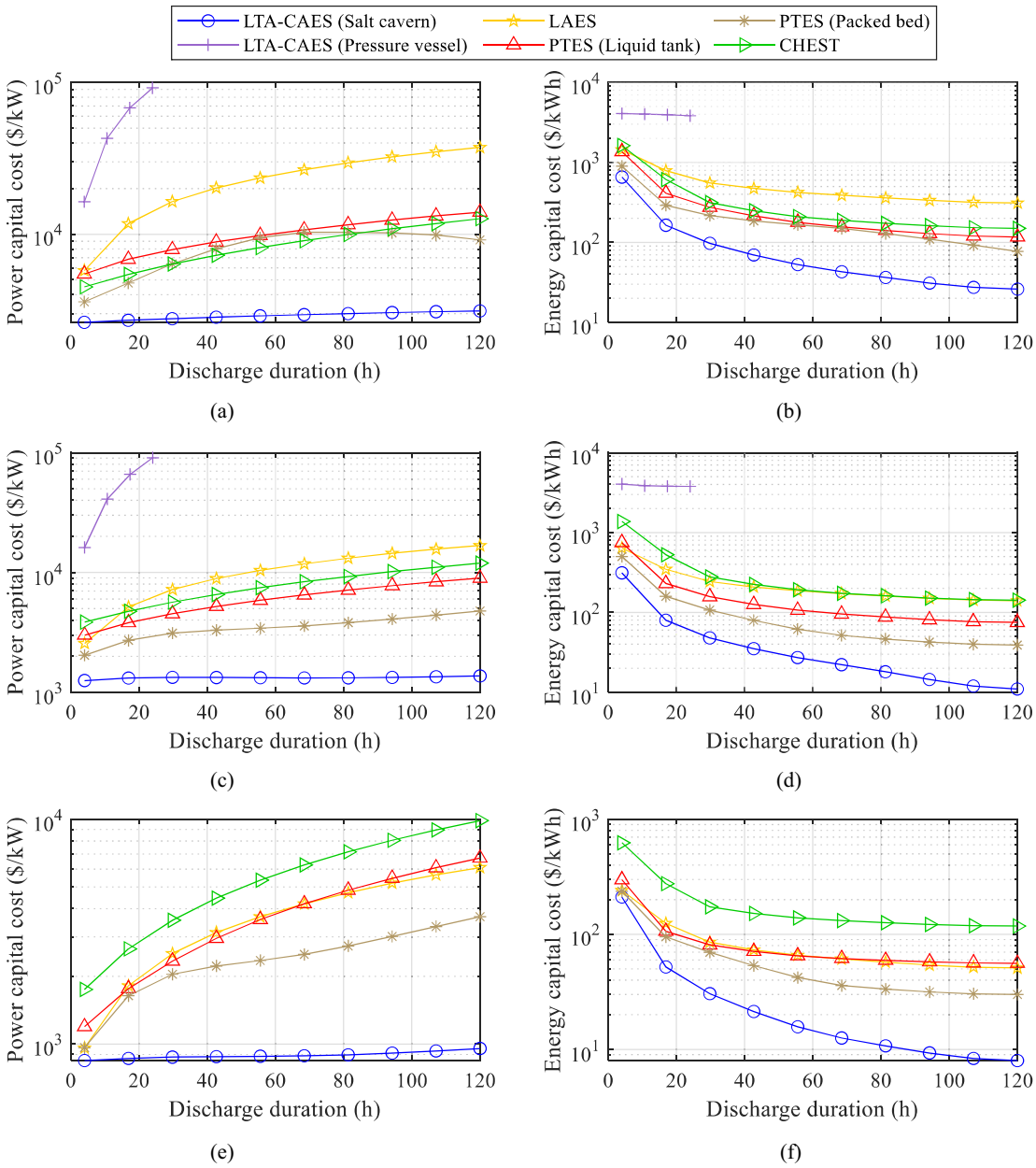

Figure 33. Thermo-economic comparison of TMES options for varying discharge duration: (a) power capital cost for a discharge power rating of 1 MW; (b) energy capital cost for a discharge power rating of 1 MW; (c) power capital cost for a discharge power rating of 10 MW; (d) energy capital cost for a discharge power rating of 10 MW; (e) power capital cost for a discharge power rating of 300 MW; (f) energy capital cost for a discharge power rating of 300 MW.

4.2.3.2. Component cost breakdown

Although the allocation of component costs of TMES systems can be significantly affected by the ratio between discharge power rating and discharge duration, an indication of these costs is presented here utilizing the thermo-economic models for systems designed for a discharge power rating of 100 MW and a discharge duration of 8 h, which was selected because it is an intermediate value among the range of sizes in table 4 and because it is a point of overlap for all of the described systems. These results are shown in figure 34.

The capital cost breakdown of LTA-CAES and LAES systems shows that the most significant impact on the share is represented by the cost associated with the heat exchangers. In the case of the LTA-CAES system, this is attributed to the significant number of heat exchangers that are required to achieve fast cycling capabilities and high efficiencies [39]. In the case of LAES, on the other hand, the heat exchanger cost takes into account also the cold box, a complex multi-stream heat exchanger implemented in the air liquefier. It is worth to underline that, aside from turbines and compressors that account for 21% and 15% of the total capital cost of the LAES system, respectively, the costs of the liquid-air tank and the two additional TES

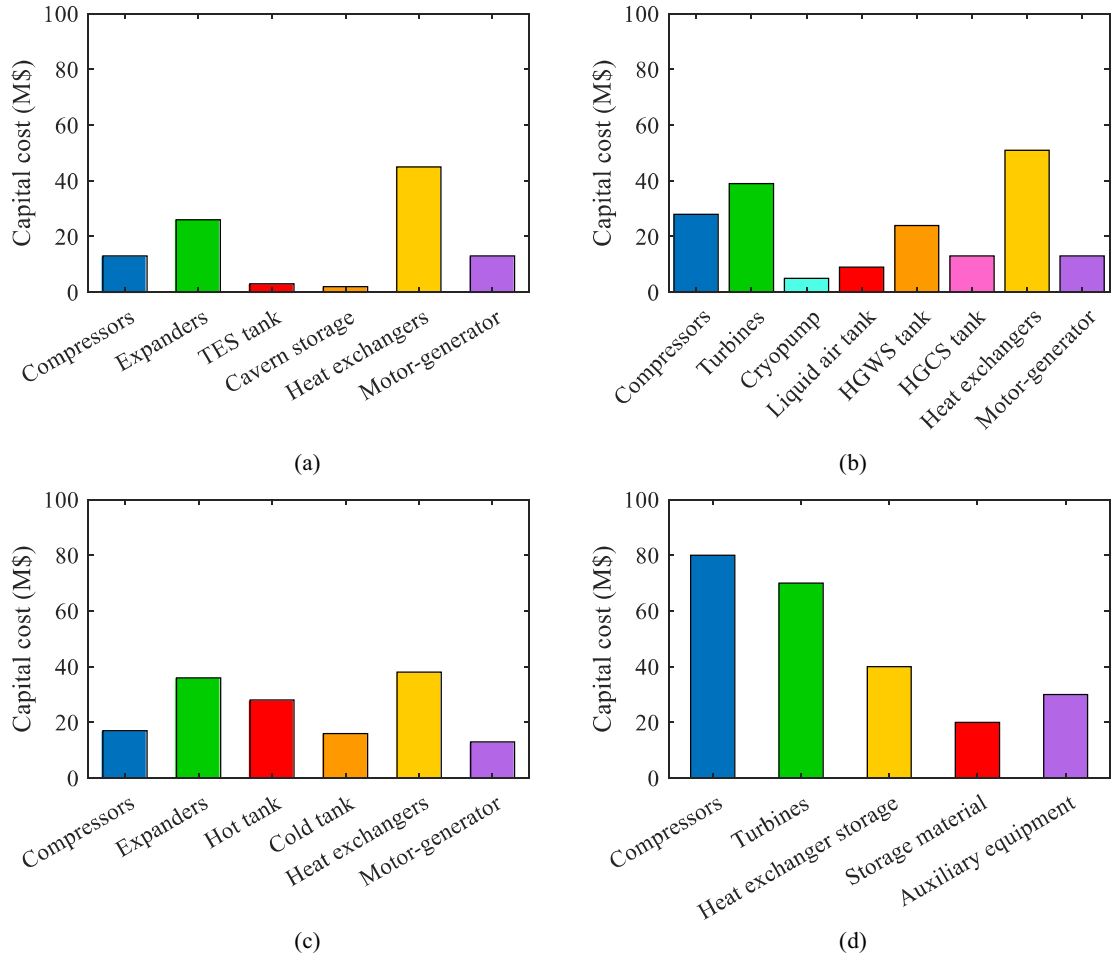

Figure 34. Component cost breakdown of TMES systems for a discharge power rating of 100 MW and a discharge duration of 8 h: (a) LTA-CAES system (salt cavern available); (b) LAES system; (c) liquid-tank Joule–Brayton PTES system; and (d) CHEST system.

systems (HGCS and HGWS) have a significant impact, accounting for almost 25% of the total. For Joule–Brayton PTES systems based on liquid-tank storage, capital costs are evenly divided between the machinery and the storage components. It is notable that the fluids for liquid storage are reasonably expensive and dominate the storage cost for PTES with liquid storage. Lastly, the costs of the CHEST system are dominated by the power block and the engines. The thermal store has a cost share of less than 25%. Especially for long charging/discharging cycles, active PCM storage is attractive since increasing the energy capacity affects only the amount of storage material required and not the capital costs of the power cycle.

4.2.3.3. Power density as a function of discharge duration

The thermodynamic models of the LTA-CAES, standalone LAES, Joule–Brayton PTES and CHEST systems are used here to determine the variation of power density with discharge duration. The reason for this analysis is that the definition of power density involves a hidden representation of the chosen rated discharge duration, which can vary widely within any given type of PTES system since power is independent from energy capacity. This means that the values reported in table 5 are estimates and a like-to-like comparison based on power density should involve equal discharge durations, as demonstrated in figure 35. It is worth highlighting that it is here assumed that the volume of storage required is almost proportional to the system's discharge power rating, which means that power density is not a function of the latter.

Figure 35 shows the high dependence of power density of TMES systems on discharge duration. At a discharge duration of 4 h, the power density of LAES reaches >15 kW m^{-3}, which is higher than the other TMES options. At this discharge duration, the power density of packed-bed Joule–Brayton PTES and CHEST systems is also high (12 kW m^{-3}), while liquid-tank PTES systems require a larger storage space and therefore the power density is significantly lower (4 kW m^{-3}). As the duration increases, the power density shows to drop significantly for all systems. At a duration of 24 h, the power density of LAES is about

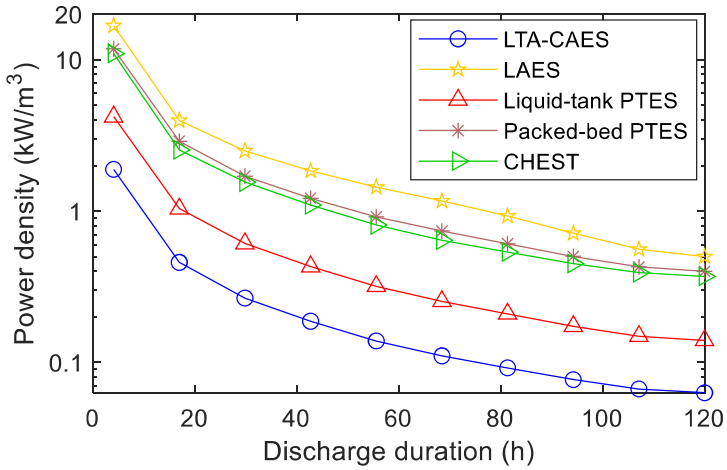

Figure 35. Power density as a function of discharge duration for four TMES systems: (a) LTA-CAES system; (b) LAES system; (c) liquid-tank Joule–Brayton PTES system; (d) packed-bed Joule–Brayton PTES system; and (e) CHEST system.

3 kW m^{-3}, while for all other systems it is below 2 kW m^{-3}. At all discharge durations, LTA-CAES shows the lowest power density due to the significant space required to store the compressed air.

4.3. Beyond pumped-hydro energy storage and batteries

In future energy systems with high shares of renewable energy, it is necessary to ensure the security of energy supply. The intermittency of renewable sources means that balancing the grid with peaking power plants (plants that run only when there is not enough supply) would involve significant investment and operating costs, increasing the overall costs of penetrating renewable energy in the energy system. On the other hand, TMES systems can be used as a promising alternative to PHES and battery systems to ensure the security of supply at low additional cost.

PHES systems involve very low energy capital costs (5–100 \$ kWh^{-1}), however TMES systems have been shown not to be far from these values. Especially for medium/long-duration (>24 h) applications, the competitiveness of TMES systems is high, with the energy capital cost being lower than 100 \$ kWh^{-1} for any discharge power rating for CAES (when an air-tight chamber is available), while for discharge power ratings higher than 10 MW, the capital cost is: (a) lower than 100 \$ kWh^{-1} for Joule–Brayton PTES; (b) about 150–400 \$ kWh^{-1} for PTES systems based on the CHEST concept; and (c) 100–300 \$ kWh^{-1} for LAES. PTES systems based on CO_2 cycles, which have a low TRL, in the range of 2–4, also show promising costs (figure 28, section 4.1). Even though the power capital cost of VRB flow batteries is low (~1000 \$ kW^{-1} compared to about 3000 \$ kW^{-1} of PHES, Li-ion batteries and most TMES systems), their energy capital cost (~600 \$ kWh^{-1}) is significantly higher than the mentioned values for TMES systems. Li-ion batteries also face significantly higher energy capital costs (600–3800 \$ kWh^{-1}).

The power and energy density of TMES systems are both significantly higher than PHES systems. For example, LAES and PTES systems based on the CHEST concept have energy densities in the range of 50–80 kWh m^{-3} and 40–100 kWh m^{-3}, respectively. This is promising performance with respect to this performance indicator, which is about 3–25 times higher than CAES and 25–160 times higher than PHES. PTES systems based on the Joule–Brayton cycle also have high energy densities (20–50 kWh m^{-3}), which are similar to those of VRB flow batteries (10–60 kWh m^{-3}). Li-ion batteries have dominant power and energy densities (1500–10 000 kW m^{-3} and 200–500 kWh m^{-3}, respectively) compared to all above systems, but they are limited to low-duration (<10 h) storage applications.

Furthermore, while the focus of storage development has long been on electricity from renewables, there is a growing interest in heat or cold delivered by renewable sources. The area of applications for TMES concepts can be increased, since these storage systems might be also applied for the energy management of smaller-sized units like shopping malls, data centres or hospitals. If heat is a useful output of the system, the requirements regarding the efficiencies and costs of the components of TMES systems can be reduced, supporting their wider deployment.

In general, TMES systems have been shown to be competitive both in terms of technical and economic characteristics compared to PHES and battery systems. They are at an earlier stage of development and, thus, have significant potential for further improvements arising, amongst other, from the evolution of key components (e.g. compression and expansion devices). It is also important to highlight the critical aspects concerning the ecological footprint of PHES and battery systems. Although PHES systems involve long

lifetime (∼60 years), their dependence on geographical location and the associated environmental concerns cause public acceptance issues and therefore lengthy permission procedures. Batteries have significantly short lifetime (10–15 years) which means they require systematic replacement and are associated with disposal and recycling issues. TMES systems can also face ecological footprint concerns: several of these systems involve storing energy at very high temperatures or pressures, which means there can be significant safety requirements which may limit where they can be placed and cause public acceptance issues. However, while there are no scientific results about the footprint of TMES systems, the requirement for less space, the long lifetime (∼30 years), the lower dependence on geographical features and the fact that they involve no toxic chemicals means that the footprint of these systems can be significantly lower.

5. Closing remarks and future perspectives

TMES systems are a class of electricity storage technologies suitable for medium/large-scale and medium/long-duration storage. In this paper, we reviewed TMES systems by focusing on a number of important TMES concepts that have been proposed and investigated in the literature and commercially, namely CAES, LAES and PTES. A synopsis was provided of their underlying thermodynamic and other (e.g. thermal) design and operational principles, variants and respective technical and economic characteristics thereof, corresponding advantages and disadvantages, and an overview was provided of recent progress, innovation and research focused on the further development and application of these systems.

A comprehensive thermo-economic analysis and comparison of the aforementioned TMES technologies was also conducted, capturing their competitiveness relative to each other and also relative to three other commonly referenced large-scale benchmark electricity storage solutions, namely PHES systems, VRBs and Li-ion batteries. This analysis and the resulting thermo-economic comparisons were based on a unified framework and common assumptions, allowing us to capture the recent evolution of the performance of the various TMES options more accurately, both in terms of performance and cost, and using a consistent set of performance and cost metrics, in a way that has not been previously reported in the literature. The early stage of TMES technology development means that cost information is limited. To overcome this challenge, component-costing models were developed as part of the framework, based on components/machines similar to those considered here, and using consistent cost correlations. Furthermore, it is known that the key technical and economic characteristics of these systems are functions of system size, so a fair like-to-like comparison requires a consideration of systems at equal sizes, and with equal discharge power ratings and durations. Therefore, the developed framework involves two stages of analysis: (a) it first assesses and compares different TMES systems at the sizes, i.e. discharge power ratings and durations, intended by their respective manufacturers/developers; and (b) it then extends the comparison by performing thermo-economic comparisons over a range of size, power ratings and durations, providing a holistic view of the ranges for which each system shows a high competitiveness.

CAES is the most commercially mature type of TMES system. Concepts based on D-CAES have proven to be a reliable and long-lifetime large-scale electricity storage option. A-CAES systems aim to store the thermal energy associated with compression and have been shown to achieve higher round-trip efficiencies (∼65% compared to ∼55% for D-CAES), while eliminating the dependency for thermal energy input, which conventionally comes from the combustion of a fossil fuel. I-CAES is a new type of CAES system, which shows good potential with estimated ultimate efficiencies in the order of 80%. The concept of storing energy in the form of air but by liquifying this rather than compressing a gaseous phase forms the motivation for the concept of LAES. Although efficiencies had been relatively low in the past (∼45%), recent progress suggests a potential for round-trip efficiency advances in the range of 10%–25%. PTES systems, which have several variants including concepts based on the Joule–Brayton cycle and the employment of liquid-tank or packed-bed thermal storage, concepts based on CO_2 cycles and concepts based on Rankine cycles (CHEST), have also been gaining increased attention recently. The type of cycle (closed/open) and thermal storage method along with the choice of compression/expansion machinery, which is a particularly important component of these systems, strongly affect their performance, with theoretical round-trip efficiencies predicted in the range 50%–70%.

TMES options target high power ratings (0.5–300 MW) and discharge durations that can be longer than 24 h. LAES concepts have high energy densities (50–80 kWh m^{-3}) and can target applications that involve discharge durations longer than 5 d, while PTES concepts are also associated with high energy densities (10–50 kWh m^{-3}) and can target similar discharge durations. Battery-based technologies cannot compete with these systems in applications where storage durations beyond 10–15 h are required, in which is a core advantage of TMES systems, as is the fact that by their nature TMES systems benefit strongly from economies of scale.

When an air-tight chamber is available, CAES systems show significantly lower power and energy capital costs than the rest of the TMES options at all considered scales. At small scales, i.e. small power ratings and for small discharge durations (∼1 MW, 4 h), CAES concepts are associated with an energy capital cost of about 600 \$ kWh^{-1}, which is less than half of other TMES options at this scale, while at larger-scales (300 MW, 120 h), this can drop by on order of magnitude to as low as 5 \$ kWh^{-1}. However, CAES systems are generally associated with low energy densities relative to other TMES technologies as well as important geographical constraints, which means that their deployment potential is limited and location-dependant. In this respect they are similar to PHES systems, which also involve low costs and equivalent constraints, compared to which CAES systems have similar energy capital costs and lower (by a factor of 2) power capital costs. At longer discharge durations, Joule–Brayton PTES systems appear as a promising alternative to CAES where location restrictions apply, with predicted energy capital costs that drop below 100 \$ kWh^{-1} at almost all discharge powers investigated in this work (1–300 MW). Similarly, for longer duration storage (>24 h), the energy capital cost of LAES systems also drops below 100 \$ kWh^{-1}, however, this is generally the case for larger systems (>50 MW); for systems with smaller power ratings that this, LAES systems exhibit projected energy capital costs in the range 100–300 \$ kWh^{-1}. Both the PTES and LAES energy capital costs are higher than those associated with conventional PHES, but lower than those of flow battery systems.

The future perspectives of TMES systems are mainly linked to research and development actions aimed at further increasing the value of the round-trip efficiency and system cost that may jeopardize the economic feasibility of energy storage investments and projects. This, in turn, depends strongly on the development (either innovation or evolution) of higher-performance and lower-cost components. From a component perspective, for example, the isothermal compression required in I-CAES systems can be also applied to LAES in order to increase this system's air-compression process efficiency. In addition, LAES performance has been shown to be significantly affected by the thermal performance of its sub-thermal energy stores, amongst which the HGCS has been identified as being, by far, the most important one. A potential long-term improvement could be achieved through the development of new PCM-based materials for the HGCS, specifically able to decrease the air liquefier specific consumption by acting as a thermal buffer for the cold TES. In the case of PTES systems, the availability of high-performance reversible compression/expansion machines would be a 'game-changer', enabling significant cost reductions due to the need for fewer components. PTES which are currently at lower TRLs generally, require further experimental testing of components, particularly high-temperature compressors, thermal storage systems, and the development of appropriate control systems; these are necessary to reduce losses and therefore improve both operation and performance. Small-scale demonstrators can provide valuable information on the behaviour, operation and performance of these systems, while large-scale pilot-plants are necessary to fully demonstrate their attributes and ultimate potential.

A great advantage of TMES systems is their ability to be integrated with other external heat sources and sinks, including waste-heat sources, thus providing extended functionality, flexibility and managing multiple energy vectors beyond electricity, e.g. heat or cold. This means that these storage systems can be interesting solutions for waste-heat recovery from industrial processes, renewable heat (e.g. solar, geothermal, biomass) or/and provide heating alongside electricity for industrial, commercial or district heating/cooling applications, with synergetic benefits to multiple diverse end-users and stakeholders within wider interconnected energy systems. Efficient sector-coupling is gaining increasing importance in smart-grid applications. In such scenarios, the system costs and benefits of TMES technologies re reduced further. Additional investigations are necessary to compare the technical and economic performance of more established solutions to novel concepts and to advance the state-of-the-art. More challenging research, due to the elevated specific costs, into small-scale systems for smaller (e.g. micro-grid) applications is also ongoing; this requires significant cost, performance and optimization improvements. The interaction of large-scale electricity storage devices with the electrical grid is an important research topic, which could evaluate the impacts of TMES on the electrical system, as well as providing information on design characteristics (e.g. load cycles, ramp rates) these systems should be aiming for.

Acknowledgments

This work was supported by the UK Engineering and Physical Sciences Research Council (EPSRC) [grant numbers EP/P004709/1, EP/S032622/1, EP/R045518/1, and EP/P003605/1], and by the UK Natural Environment Research Council (NERC) [grant number NE/L002515/1]. The authors would also like to acknowledge the Science and Solutions for a Changing Planet Doctoral Training Partnership (SSCP DTP). This work was authored in part by the National Renewable Energy Laboratory, operated by Alliance for Sustainable Energy LLC, for the US Department of Energy (DOE) under Contract No.

DE-AC36-08GO28308. Funding provided by US Department of Energy Office of Energy Efficiency and Renewable Energy Solar Energy Technologies Office. The views expressed in the article do not necessarily represent the views of the DOE or the US Government. The US Government retains and the publisher, by accepting the article for publication, acknowledges that the US Government retains a nonexclusive, paid-up, irrevocable, worldwide license to publish or reproduce the published form of this work, or allow others to do so, for US Government purposes. Partial support by the National Natural Science Foundation of China under Grant No. 51820105010 is appreciated. Data supporting this publication can be obtained on request from cep-lab@imperial.ac.uk.

ORCID iDs

Andreas V Olympios https://orcid.org/0000-0002-5795-0408
Joshua D McTigue https://orcid.org/0000-0003-3736-2788
Pau Farres-Antunez https://orcid.org/0000-0002-2263-2629
Alessio Tafone https://orcid.org/0000-0002-6543-5297
Alessandro Romagnoli https://orcid.org/0000-0003-1271-5479
Yongliang Li https://orcid.org/0000-0001-6231-015X
Yulong Ding https://orcid.org/0000-0001-8490-5349
Christos N Markides https://orcid.org/0000-0002-4219-1867

References

[1] Green M A 2019 Photovoltaic technology and visions for the future *Prog. Energy* **1** 013001
[2] Fragaki A, Markvart T and Laskos G 2019 All UK electricity supplied by wind and photovoltaics—the 30–30 rule *Energy* **169** 228–37
[3] REN21 2019 Renewables 2019: Global status report (www.ren21.net/wp-content/uploads/2019/05/gsr_2019_full_report_en.pdf)
[4] Hansen K, Breyer C and Lund H 2019 Status and perspectives on 100% renewable energy systems *Energy* **175** 471–80
[5] Rogelj J, Luderer G, Pietzcker R C, Kriegler E, Schaeffer M, Krey V and Riahi K 2015 Energy system transformations for limiting end-of-century warming to below 1.5 °C *Nat. Clim. Change* **5** 519–27
[6] Luo X, Wang J, Dooner M and Clarke J 2015 Overview of current development in electrical energy storage technologies and the application potential in power system operation *Appl. Energy* **137** 511–36
[7] Chen H, Cong T N, Yang W, Tan C, Li Y and Ding Y 2009 Progress in electrical energy storage system: a critical review *Prog. Nat. Sci.* **19** 291–312
[8] World Energy Council 2016 E-storage: shifting from cost to value—wind and solar applications
[9] International Energy Association 2019 Tracking energy integration
[10] World Energy Council 2019 Energy storage monitor: latest trends in energy storage
[11] Gallo A B, Simões-Moreira J R, Costa H K M, Santos M M and Moutinho dos Santos E 2016 Energy storage in the energy transition context: a technology review *Renew. Sustain. Energy Rev.* **65** 800–22
[12] Siddiqui O and Dincer I 2017 Comparative assessment of the environmental impacts of nuclear, wind and hydro-electric power plants in Ontario: a life cycle assessment *J. Clean. Prod.* **164** 848–60
[13] Zablocki A 2019 Energy storage: fact sheet (Environmental and Energy Study Institute)
[14] Colthorpe A 2018 China's biggest flow battery project so far is underway with hundreds more megawatts to come (www.energy-storage.news/news/chinas-biggest-flow-battery-project-so-far-is-underway-with-hundreds-more-m)
[15] Nguyen T and Savinell R F 2010 Flow batteries *Electrochem. Soc. Interface* **19** 54–56
[16] Shi Y, Eze C, Xiong B, He W, Zhang H, Lim T M, Ukil A and Zhao J 2019 Recent development of membrane for vanadium redox flow battery applications: a review *Appl. Energy* **238** 202–24
[17] Steinmann W D 2017 Thermo-mechanical concepts for bulk energy storage *Renew. Sustain. Energy Rev.* **75** 205–19
[18] Georgiou S, Shah N and Markides C N 2018 A thermo-economic analysis and comparison of pumped-thermal and liquid-air electricity storage systems *Appl. Energy* **226** 1119–33
[19] Georgiou S, Aunedi M, Strbac G and Markides C N 2020 On the value of liquid-air and pumped-thermal electricity storage systems in low-carbon electricity systems *Energy* **193** 116680
[20] Benato A and Stoppato A 2018 Pumped thermal electricity storage: a technology overview *Therm. Sci. Eng. Prog.* **6** 301–15
[21] Budt M, Wolf D, Span R and Yan J 2016 A review on compressed air energy storage: basic principles, past milestones and recent developments *Appl. Energy* **170** 250–68
[22] Steinmann W D, Jockenhöfer H and Bauer D 2020 Thermodynamic analysis of high-temperature Carnot battery concepts *Energy Technol.* **8** 1900895
[23] Venkataramani G, Parankusam P, Ramalingam V and Wang J 2016 A review on compressed air energy storage—a pathway for smart grid and polygeneration *Renew. Sustain. Energy Rev.* **62** 895–907
[24] Dinelli G, Lozza G and Macchi E 1988 A feasibility study of CAES plants for peak load generation *Proc: 23rd Intersociety Energy Conversion Engineering Conf. (IECEC)* (Denver, CO: American Society of Mechanical Engineers (ASME)) pp 417–24
[25] Borzea C, Vlăducă I, Ionescu D, Petrescu V, Niculescu F, Nechifor C, Vătășelu G and Hanek M 2019 Compressed air energy storage installation for renewable energy generation *E3S Web Conf.* **112** 02010
[26] Gay F W 1948 Means for storing fluids for power generation *U.S. Patent* 2433896
[27] He W and Wang J 2018 Optimal selection of air expansion machine in compressed air energy storage: a review *Renewable Sustain. Energy Rev.* **87** 77–95
[28] Jafarizadeh H, Soltani M and Nathwani J 2020 Assessment of the Huntorf compressed air energy storage plant performance under enhanced modifications *Energy Convers. Manage.* **209** 112662

[29] Ishihata T 1997 Underground compressed air storage facility for CAES-G/T power plant utilizing an airtight lining *News J. Int. Soc. Rock Mech.* **5** 17–21
[30] Denholm P 2006 Improving the technical, environmental and social performance of wind energy systems using biomass-based energy storage *Renew. Energy* **31** 1355–70
[31] Safaei H, Keith D W and Hugo R J 2013 Compressed air energy storage (CAES) with compressors distributed at heat loads to enable waste heat utilization *Appl. Energy* **103** 165–79
[32] Safaei H and Keith D W 2014 Compressed air energy storage with waste heat export: an Alberta case study *Energy Convers. Manage.* **78** 114–24
[33] Bieber M, Marquardt R and Moser P 2010 The ADELE project: development of an adiabatic CAES plant towards marketability *Proc: 5th Int. Renewable Energy Storage Conf.* (*Bonn, Munich*)
[34] Barbour E, Mignard D, Ding Y and Li Y 2015 Adiabatic compressed air energy storage with packed bed thermal energy storage *Appl. Energy* **155** 804–15
[35] Sciacovelli A, Li Y, Chen H, Wu Y, Wang J, Garvey S and Ding Y 2017 Dynamic simulation of adiabatic compressed air energy storage (A-CAES) plant with integrated thermal storage—link between components performance and plant performance *Appl. Energy* **185** 16–28
[36] Hartmann N, Vöhringer O, Kruck C and Eltrop L 2012 Simulation and analysis of different adiabatic compressed air energy storage plant configurations *Appl. Energy* **93** 541–8
[37] Wolf D and Budt M 2014 LTA-CAES—a low-temperature approach to adiabatic compressed air energy storage *Appl. Energy* **125** 158–64
[38] Luo X, Wang J, Krupke C, Yue W, Sheng Y, Li J, Xu Y, Wang D, Miao S and Chen H 2016 Modelling study, efficiency analysis and optimisation of large-scale adiabatic compressed air energy storage systems with low-temperature thermal storage *Appl. Energy* **162** 589–600
[39] Yang K, Zhang Y, Li X and Xu J 2014 Theoretical evaluation on the impact of heat exchanger in advanced adiabatic compressed air energy storage system *Energy Convers. Manage.* **86** 1031–44
[40] Liu J and Wang J 2016 A comparative research of two adiabatic compressed air energy storage systems *Energy Convers. Manage.* **108** 566–78
[41] Guo H, Xu Y, Zhang Y, Liang Q, Tang H, Zhang X, Zuo Z and Chen H 2019 Off-design performance and an optimal operation strategy for the multistage compression process in adiabatic compressed air energy storage systems *Appl. Therm. Eng.* **149** 262–74
[42] Peng H, Yang Y, Li R and Ling X 2016 Thermodynamic analysis of an improved adiabatic compressed air energy storage system *Appl. Energy* **183** 1361–73
[43] Guo Z, Deng G, Fan Y and Chen G 2016 Performance optimization of adiabatic compressed air energy storage with ejector technology *Appl. Therm. Eng.* **94** 193–7
[44] Odukomaiya A, Abu-Heiba A, Gluesenkamp K R, Abdelaziz O, Jackson R K, Daniel C, Graham S, and Momen A M 2016 Thermal analysis of near-isothermal compressed gas energy storage system *Appl. Energy* **179** 948–60
[45] Yirka B 2013 SustainX builds 1.5 MW isotherm compressed air energy storage system (available at: https://phys.org/news/2013-09-sustainx-mw-isotherm-compressed-air.html)
[46] Lemofouet-Gatsi S 2006 Investigation and optimisation of hybrid electricity storage systems based on compressed air and supercapacitors EPFL Thesis (https://doi.org/10.5075/epfl-thesis-3628)
[47] Li P Y, Van de Ven J D and Sancken C 2007 Open accumulator concept for compact fluid power energy storage *Proc: Int. Mechanical Engineering Congress and Exposition (IMECE)* (Seattle, WA: American Society of Mechanical Engineers (ASME))
[48] Li P Y, Simon T W, Van de Ven J D and Crane S E 2011 Compressed air energy storage for offshore wind turbines *Proc: Int. Fluid Power Exhibition (IFPE)* (*Las Vegas, United States*)
[49] Park J, Ro P I, Lim S D, Mazzoleni A P, Quinlan B and Carolina N 2012 Analysis and optimization of a quasi-isothermal compression and expansion cycle for ocean compressed air energy storage (OCAES) *Proc: 2012 Oceans*, (*Hampton Roads, United States*)
[50] Lim S D, Mazzoleni A P, Park J, Ro P I and Quinlan B 2012 Conceptual design of ocean compressed air energy storage system *Proc: 2012 Oceans* (*Hampton Roads, United States*)
[51] Coney M W, Stephenson P, Malmgren A, Linnemann C and Morgan R E 2002 Development of a reciprocating compressor using water injection to achieve quasi-isothermal compression *Proc: Int. Compressor Engineering Conf.* (*West Lafayette, United States*)
[52] Zhang X, Xu Y, Zhou X, Zhang Y, Li W, Zuo Z, Guo H, Huang Y and Chen H 2018 A near-isothermal expander for isothermal compressed air energy storage system *Appl. Energy* **225** 955–64
[53] Iglesias A and Favrat D 2014 Innovative isothermal oil-free co-rotating scroll compressor–expander for energy storage with first expander tests *Energy Convers. Manage.* **85** 565–72
[54] McBride T, Bell A and Kepshire D 2013 *ICAES innovation: foam-based heat exchange* (Seabrook: SustainX)
[55] Li P Y and Saadat M 2016 An approach to reduce the flow requirement for a liquid piston near-isothermal air compressor/expander in a compressed air energy storage system *IET Renew. Power Gener.* **10** 1506–14
[56] Heidari M, Mortazavi M and Rufer A 2017 Design, modeling and experimental validation of a novel finned reciprocating compressor for isothermal compressed air energy storage applications *Energy* **140** 1252–66
[57] Castellani B, Presciutti A, Filipponi M, Nicolini A and Rossi F 2015 Experimental investigation on the effect of phase change materials on compressed air expansion in CAES plants *Sustainability* **7** 9773–86
[58] Nielsen L and Leithner R 2009 Dynamic simulation of an innovative compressed air energy storage plant—detailed modelling of the storage cavern *WSEAS Trans. Power Syst.* **4** 253–63
[59] Kim Y M and Favrat D 2010 Energy and exergy analysis of a micro-compressed air energy storage and air cycle heating and cooling system *Energy* **35** 213–20
[60] Mazloum Y, Sayah H and Nemer M 2017 Dynamic modeling and simulation of an isobaric adiabatic compressed air energy storage (IA-CAES) system *J. Energy Storage* **11** 178–90
[61] Tweed K 2015 Toronto hydro pilots world's first offshore compressed-air energy storage project (www.greentechmedia.com/articles/read/toronto-hydro-pilots-worlds-first-offshore-compressed-air-energy-storage)
[62] Pimm A J, Garvey S D and De Jong M 2014 Design and testing of energy bags for underwater compressed air energy storage *Energy* **66** 496–508
[63] Cheung B C, Carriveau R and Ting D S 2014 Parameters affecting scalable underwater compressed air energy storage *Appl. Energy* **134** 239–47

[64] Morgan R, Nelmes S, Gibson E and Brett G 2015 An analysis of a large-scale liquid air energy storage system *Proc. Inst. Civil Eng.—Energy* **168** 135–44
[65] Kim J, Noh Y and Chang D 2018 Storage system for distributed-energy generation using liquid air combined with liquefied natural gas *Appl. Energy* **212** 1417–32
[66] Alyami H H and Williams R 2015 Study and evaluation of liquid air energy storage technology for a clean and secure energy future challenges and opportunities for Alberta wind energy industry *Am. J. Eng. Res.* **4** 41–54
[67] Tafone A, Romagnoli A, Li Y and Borri E 2016 Techno-economic analysis of a liquid air energy storage (LAES) for cooling application in hot climates *Proc: 8th Int. Conf. on Applied Energy* (*Beijing, China*)
[68] The Carbon Trust 2015 The emerging cold economy (www.carbontrust.com/resources/the-emerging-cold-economy)
[69] Dearman Company. The cold economy 2014 (http://dearman.co.uk/wp-content/uploads/2016/05/cold-economy-document-.pdf)
[70] Sciacovelli A, Smith D, Navarro H, Li Y and Ding Y 2016 Liquid air energy storage—operation and performance of the first pilot plant in the world *Proc: ECOS 2016: Int. Conf. on Efficiency, Cost, Optimisation, Simulation and Environmental Impact of Energy Systems* (*Portorož, Slovenia*)
[71] Shepherd D G 1974 A low-pollution on-site, energy storage system for peak-power supply *Proc: ASME*
[72] Smith E M 1977 Storage of electrical energy using supercritical liquid air *Inst. Mech. Eng.* **191** 289–98
[73] Kishimoto K, Hasegawa K and Asano T 1998 Development of generator of liquid air storage energy system Mitsubishi Heavy Industries Ltd *Tech. Rev.* **35** 117–20
[74] Chino K and Araki H 2000 Evaluation of energy storage method using liquid air *Heat Transf. Res.* **29** 347–57
[75] Highview Power 2020 Mission possible: a world powered by 100% renewable energy (www.highviewpower.com)
[76] Morgan R, Nelmes S, Gibson E and Brett G 2015 Liquid air energy storage—analysis and first results from a pilot scale demonstration plant *Appl. Energy* **137** 845–53
[77] Highview Power 2018 Highview Power launches world's first grid-scale liquid air energy storage plant (www.highviewpower.com/news_announcement/world-first-liquid-air-energy-storage-plant)
[78] Chen H, Ding Y, Peters T and Berger F 2007 A method of storing energy and a cryogenic energy storage system WO2007217133
[79] Highview Power 2019 Highview Power to develop multiple cryogenic energy storage facilities in the UK and to build Europe's largest storage system (www.highviewpower.com/news_announcement/highview-power-to-develop-multiple-cryogenic-energy-storage-facilities-in-the-uk-and-to-build-europes-largest-storage-system)
[80] Highview Power 2019 Highview Power and Encore Renewable Energy to co-develop the first long duration, liquid air energy storage system in the United States (www.highviewpower.com/news_announcement/highview-power-and-encore-renewable-energy-to-co-develop-the-first-long-duration-liquid-air-energy-storage-system-in-the-united-states)
[81] Ameel B, T'Joen C, De Kerpel K, De Jaeger P, Huisseune H, Van Belleghem M and De Paepe M 2013 Thermodynamic analysis of energy storage with a liquid air Rankine cycle *Appl. Therm. Eng.* **52** 130–40
[82] Guizzi G L, Manno M, Tolomei L M and Vitali R M 2015 Thermodynamic analysis of a liquid air energy storage system *Energy* **2015** 1639–47
[83] Xue X D, Wang S X, Zhang X L, Cui C, Chen L B, Zhou Y and Wang J J 2015 Thermodynamic analysis of a novel liquid air energy storage system *Phys. Procedia* **67** 733–8
[84] Sciacovelli A, Vecchi A and Ding Y 2017 Liquid air energy storage (LAES) with packed bed cold thermal storage—from component to system level performance through dynamic modelling *Appl. Energy* **190** 84–98
[85] Peng H, Shan X, Yang Y and Ling X 2018 A study on performance of a liquid air energy storage system with packed bed units *Appl. Energy* **211** 126–35
[86] Chen H, Tan C, Liu J and Xu Y 2015 *U.S. Patent No* 9217423
[87] Comodi G, Carducci F, Sze J Y, Balamurugan N and Romagnoli A 2017 Storing energy for cooling demand management in tropical climates: a techno-economic comparison between different energy storage technologies *Energy* **121** 676–94
[88] Ahmad A, Al-Dadah R and Mahmoud S 2016 Liquid nitrogen energy storage for air conditioning and power generation in domestic applications *Energy Convers. Manage.* **128** 34–43
[89] Al-Zareer M, Dincer I and Rosen M A 2017 Analysis and assessment of novel liquid air energy storage system with district heating and cooling capabilities *Energy* **141** 792–802
[90] She X, Peng X, Nie B, Leng G, Zhang X, Weng L, Tong L, Zheng L, Wang L and Ding Y 2017 Enhancement of round trip efficiency of liquid air energy storage through effective utilization of heat of compression *Appl. Energy* **206** 1632–42
[91] Tafone A, Ding Y, Li Y, Xie C and Romagnoli A 2020 Levelised cost of storage (LCOS) analysis of liquid air energy storage system integrated with organic Rankine cycle *Energy* **198** 117275
[92] Tafone A, Borri E, Comodi G, van den Broek M and Romagnoli A 2018 Liquid air energy storage performance enhancement by means of organic Rankine cycle and absorption chiller *Appl. Energy* **228** 1810–21
[93] Peng X, She X, Cong L, Zhang T, Li C, Li Y, Wang L, Tong L and Ding Y 2018 Thermodynamic study on the effect of cold and heat recovery on performance of liquid air energy storage *Appl. Energy* **221** 86–99
[94] Kantharaj B, Garvey S and Pimm A 2015 Compressed air energy storage with liquid air capacity extension *Appl. Energy* **157** 152–64
[95] Farres-Antunez P, Xue H and White A J 2018 Thermodynamic analysis and optimisation of a combined liquid air and pumped thermal energy storage cycle *J. Energy Storage* **18** 90–102
[96] Li Y, Chen H and Ding Y 2010 Fundamentals and applications of cryogen as a thermal energy carrier: a critical assessment *Int. J. Therm. Sci.* **49** 941–9
[97] Hamdy S, Moser F, Morosuk T and Tsatsaronis G 2019 Exergy-based and economic evaluation of liquefaction processes for cryogenics energy storage *Energies* **12** 493
[98] Borri E, Tafone A, Romagnoli A and Comodi G 2017 A preliminary study on the optimal configuration and operating range of a 'microgrid scale' air liquefaction plant for liquid air energy storage *Energy Convers. Manage.* **143** 275–85
[99] Guo H, Xu Y, Chen H and Zhou X 2016 Thermodynamic characteristics of a novel supercritical compressed air energy storage system *Energy Convers. Manage.* **115** 167–77
[100] ESCN News 2016 Project 'R&D and demonstration of supercritical compressed air energy storage system' passed the technical acceptance (www.escn.com.cn/news/show-324451.html)
[101] Wang J, Lu K, Ma L, Wang J, Dooner M, Miao S, Li J and Wang D 2017 Overview of compressed air energy storage and technology development *Energies* **10** 991

[102] Borri E, Tafone A, Comodi G and Romagnoli A 2017 Improving liquefaction process of microgrid scale liquid air energy storage (LAES) through waste heat recovery (WHR) and absorption chiller *Energy Procedia* **143** 699–704
[103] Zhang T, Zhang X L, He Y L, Xue X D and Mei S W 2020 Thermodynamic analysis of hybrid liquid air energy storage systems based on cascaded storage and effective utilization of compression heat *Appl. Therm. Eng.* **164** 114526
[104] Cetin T H, Kanoglu M and Yanikomer N 2019 Cryogenic energy storage powered by geothermal energy *Geothermics* **77** 34–40
[105] Pimm A J, Garvey S D and Kantharaj B 2015 Economic analysis of a hybrid energy storage system based on liquid air and compressed air *J. Energy Storage* **4** 24–35
[106] McTigue J D 2016 Analysis and optimisation of thermal energy storage *PhD Thesis* University of Cambridge (https://doi.org/10.17863/CAM.7084)
[107] Weissenbach B 1979 Thermal energy storage device EP/0003980 A1
[108] Ruer J 2008 Installation and methods for storing and recovering electrical energy WO/2008/148962 A2
[109] The Engineer 2019 Newcastle University connects first grid-scale pumped heat energy storage system (www.theengineer.co.uk/grid-scale-pumped-heat-energy-storage)
[110] MacNaughten J and Howes J S 2009 Energy storage WO/2009/044139 A2
[111] Laughlin R B, Larochelle P and Cizek N 2015 Systems and methods for energy storage and retrieval *US* 2015/0260463 A1
[112] Laughlin R B 2016 Adiabatic salt energy storage *US* 2016/0298455 A1.
[113] McTigue J D, Farres-Antunez P, Ellingwood K, Neises T and White A J 2019 Pumped thermal electricity storage with supercritical CO_2 cycles and solar heat input *Proc: SolarPACES* (*Daegu, South Korea*)
[114] White A J, Parks G and Markides C N 2013 Thermodynamic analysis of pumped thermal electricity storage *Appl. Therm. Eng.* **53** 291–8
[115] Laughlin R B 2017 Pumped thermal grid storage with heat exchange *J. Renewable Sustainable Energy* **9** 044103
[116] Kim Y M, Shin D G, Lee S Y and Favrat D 2013 Isothermal transcritical CO_2 cycles with TES (thermal energy storage) for electricity storage *Energy* **49** 484–501
[117] Thess A 2013 Thermodynamic efficiency of pumped heat electricity storage *Phys. Rev. Lett.* **111** 110602
[118] Guo J, Cai L, Chen J and Zhou Y 2016 Performance optimization and comparison of pumped thermal and pumped cryogenic electricity storage systems *Energy* **106** 260–9
[119] Desrues T, Ruer J, Marty P and Fourmigué J F 2010 A thermal energy storage process for large scale electric applications *Appl. Therm. Eng.* **30** 425–32
[120] McTigue J D, White A J and Markides C N 2015 Parametric studies and optimisation of pumped thermal electricity storage *Appl. Energy* **137** 800–11
[121] Howes J 2012 Concept and development of a pumped heat electricity storage device *IEEE* **100** 493–503
[122] Farres-Antunez P 2018 Modelling and development of thermo-mechanical energy storage *PhD Thesis* University of Cambridge (https://doi.org/10.17863/CAM.38056)
[123] McTigue J D, Markides C N and White A J 2018 Performance response of packed-bed thermal storage to cycle duration perturbations *J. Energy Storage* **19** 379–92
[124] Wang L, Lin X, Chai L, Peng L, Yu D and Chen H 2019 Cyclic transient behavior of the Joule-Brayton based pumped heat electricity storage: modeling and analysis *Renew. Sustain. Energy Rev.* **111** 523–34
[125] Frutschi H U 2005 Closed-cycle gas turbines: operating experience and future potential *ASME*
[126] Bruch A, Fourmigué J F and Couturier R 2014 Experimental and numerical investigation of a pilot-scale thermal oil packed bed thermal storage system for CSP power plant *Sol. Energy* **105** 116–25
[127] Fasquelle T, Falcoz Q, Neveu P and Ho J 2018 A temperature threshold evaluation for thermocline energy storage in concentrated solar power plants *Appl. Energy* **212** 1153–64
[128] Zanganeh G, Khanna R, Walser C, Pedretti A, Haselbacher A and Steinfeld A 2015 Experimental and numerical investigation of combined sensible–latent heat for thermal energy storage at 575 °C and above *Sol. Energy* **114** 77–90
[129] Crandall D M and Thacher E F 2004 Segmented thermal storage *Sol. Energy* **77** 435–40
[130] White A J, McTigue J D and Markides C N 2016 Analysis and optimisation of packed-bed thermal reservoirs for electricity storage applications *Proc. Inst. Mech. Eng. A: J. Power Energy* **230** 739–54
[131] McTigue J D and White A J 2016 Segmented packed beds for improved thermal energy storage performance *IET Renewable Power Gener.* **10** 1498
[132] Morandin M and Henchoz S 2011 Thermo-electrical energy storage: a new type of large scale energy storage based on thermodynamic cycles *Proc: World Engineers Convention* (*Geneva, Switzerland*)
[133] Farres-Antunez P and White A J 2016 Thermodynamic strategies for pumped thermal exergy storage (PTES) with liquid reservoirs *UK Energy Storage Conf.* (*Birmingham, UK*)
[134] Fernández A G, Gomez-Vidal J, Oró E, Kruizenga A, Solé A and Cabeza L F 2019 Mainstreaming commercial CSP systems: a technology review *Renew. Energy* **140** 152–76
[135] Bonk A, Braun M, Sötz V A and Bauer T 2020 Solar salt—pushing an old material for energy storage to a new limit *Appl. Energy* **262** 114535
[136] Lawton B 1987 Effect of compression and expansion on instantaneous heat transfer in reciprocating internal combustion engines *Proc. Inst. Mech. Eng. A: J. Power Proc. Eng.* **201** 175–86
[137] Mathie R, Markides C N and White A J 2014 A framework for the analysis of thermal losses in reciprocating compressors and expanders *Heat Transfer Eng.* **35(16–17** 1435–49
[138] Ma Z 2020 PHES researches in Durham University *Int. Energy Agency ECES Annex 36 on Carnot Batteries. Kick-off Web Meeting*
[139] Benato A 2017 Performance and cost evaluation of an innovative pumped thermal electricity storage power system *Energy* **138** 419–36
[140] Chen L X, Hu P, Xie M N and Wang F X 2018 Thermodynamic analysis of a high temperature pumped thermal electricity storage (HT-PTES) integrated with a parallel organic Rankine cycle (ORC) *Energy Convers. Manage.* **177** 150–60
[141] Robinson A 2017 Ultra-high temperature thermal energy storage. Part 1: concepts *J. Energy Storage* **13** 277–86
[142] Robinson A 2018 Ultra-high temperature thermal energy storage. Part 2: engineering and operation *J. Energy Storage* **18** 333–9
[143] Mercangöz M, Hemrle J, Kaufmann L, Graggen A Z and Ohler C 2012 Electrothermal energy storage with transcritical CO_2 cycles *Energy* **45** 407–15
[144] Morandin M 2012 Maréchal F, Mercangöz M, Buchter F. Conceptual design of a thermo-electrical energy storage system based on heat integration of thermodynamic cycles—part A: methodology and base case *Energy* **45** 375–85

[145] Morandin M, Maréchal F, Mercangöz M and Buchter F 2012 Conceptual design of a thermo-electrical energy storage system based on heat integration of thermodynamic cycles—part B: alternative system configurations *Energy* **45** 386–96
[146] Morandin M, Mercangöz M, Hemrle J, Maréchal F and Favrat D 2013 Thermoeconomic design optimization of a thermo-electric energy storage system based on transcritical CO_2 cycles *Energy* **58** 571–87
[147] Ayachi F, Tauveron N, Tartière T, Colasson S and Nguyen D 2016 Thermo-electric energy storage involving CO_2 transcritical cycles and ground heat storage *Appl. Therm. Eng.* **108** 1418–28
[148] Tauveron N, Macchi E, Nguyen D and Tartière T 2017 Experimental study of supercritical CO2 heat transfer in a thermo-electric energy storage based on Rankine and heat-pump cycles *Energy Procedia* **129** 939–46
[149] Wright S A, Graggen A Z and Hemrle J 2013 Control of a supercritical CO_2 electro-thermal energy storage system *Proc: ASME Turbo Expo: Turbine Technical Conf. and Exposition* (*San Antonio, United States*)
[150] Baik Y, Heo J, Koo J and Kim M 2014 The effect of storage temperature on the performance of a thermo-electric energy storage using a transcritical CO_2 cycle *Energy* **75** 204–15
[151] Abarr M, Geels B, Hertzberg J and Montoya L D 2017 Pumped thermal energy storage and bottoming system part A: concept and model *Energy* **120** 320–31
[152] Abarr M, Hertzberg J and Montoya L D 2017 Pumped thermal energy storage and bottoming system part B: sensitivity analysis and baseline performance *Energy* **119** 601–11
[153] Koen A, Farres-Antunez P and White A J 2019 A study of working fluids for transcritical pumped thermal energy storage cycles *Proc: Offshore Energy and Storage Summit (OSES)* (*Brest, France*)
[154] Marguerre F 1920 Verfahren und vorrichtung zum aufspeichern von energie *Deutsches Reich Patent DRP* 337356
[155] Steinmann W D 2014 The CHEST (compressed heat energy storage) concept for facility scale thermo mechanical energy storage *Energy* **69** 543–52
[156] Laing D, Bauer T, Breidenbach N, Hachmann B and Johnson M 2013 Development of high temperature phase-change-material storages *Appl. Energy* **109** 497–504
[157] Viking heating engines 2020 Heat booster high-temperature heat pump (www.vikingheatengines.com/heatbooster)
[158] Chester 2020 Compressed heat energy storage for energy from renewable sources: the project (www.chester-project.eu/about-chester/the-project)
[159] Henchoz S, Buchter F, Favrat D, Morandin M and Mercangöz M 2012 Thermoeconomic analysis of a solar enhanced energy storage concept based on thermodynamic cycles *Energy* **2012** 358–65
[160] Fiaschi D, Manfrida G, Petela K and Talluri L 2019 Thermo-electric energy storage with solar heat integration: exergy and exergo-economic analysis *Energies* **12** 648
[161] Farres-Antunez P, McTigue J D and White A J 2019 A pumped thermal energy storage cycle with capacity for concentrated solar power integration *Proc: Offshore Energy and Storage Summit (OSES)* (*Brest, France*)
[162] Aga V, Conte E, Carroni R, Burcker B and Ramond M 2016 Supercritical CO_2-based heat pump cycle for electrical energy storage for utility scale dispatchable renewable energy power plant *Proc: 5th Int. Symp.—Supercritical CO_2 Power Cycles* (*San Antonio, United States*)
[163] Vinnemeier P, Wirsum M, Malpiece D and Bove R 2016 Integration of heat pumps into thermal plants for creation of large-scale electricity storage capacities *Appl. Energy* **184** 506–22
[164] Geyer M 2018 Carnot batteries for the decarbonization of coal fired power plants using high temperature thermal storage technologies from solar power plants *Proc: Int. Workshop on Carnot Batteries* (*Stuttgart, Germany*)
[165] Frate G F, Antonelli M and Desideri U 2017 A novel pumped thermal electricity storage (PTES) system with thermal integration *Appl. Therm. Eng.* **121** 1051–8
[166] Jockenhofer H, Steinmann W D and Bauer D 2018 Detailed numerical investigation of a pumped thermal energy storage with low temperature heat integration *Energy* **145** 665–76
[167] Schimpf S and Span R 2015 Techno-economic evaluation of a solar assisted combined heat pump—organic Rankine cycle system *Energy Convers. Manage.* **94** 430–7
[168] Vandersickel A, Aboueldahab A and Spliethoff H 2016 Small-scale pumped heat electricity storage for decentralised combined heat and power generation: cost optimal design and operation *Proc: The 29th Int. Conf. on Efficiency, Cost, Optimization, Simulation and Environmental Impact of Energy Systems (ECOS)* (*Portorož, Slovenia*)
[169] Dumont O, Quoilin S and Lemort V 2015 Experimental investigation of a reversible heat pump/organic Rankine cycle unit designed to be coupled with a passive house to get a net zero energy building *Int. J. Refrig.* **54** 190–203
[170] Attonaty K, Pouvreau J, Deydier A, Oriol J and Stouffs P 2020 Thermodynamic and economic evaluation of an innovative electricity storage system based on thermal energy storage *Renew. Energy* **150** 1030–6
[171] Markides C N 2015 Low-concentration solar-power systems based on organic Rankine cycles for distributed-scale applications: overview and further developments *Front. Energy Res.* **3** 47
[172] Datas A, Ramos A, Martí A, Del Canizo C and Luque A 2016 Ultra-high temperature latent heat energy storage and thermophotovoltaic energy conversion *Energy* **107** 542–9
[173] Hameer S and van Niekerk J L 2015 A review of large-scale electrical energy storage *Int. J. Energy Res.* **2015** 1179–95
[174] Wolf D 2011 Methods for design and application of adiabatic compressed air energy: storage based on dynamic modeling *PhD Thesis* Fraunhofer Institute
[175] Rogers A, Henderson A, Wang X and Negnevitsky M 2014 Compressed air energy storage: thermodynamic and economic review *IEEE PES General Meeting | Conf. and Exposition* (*Washington, United States*)
[176] Bollinger B 2015 Technology performance report: SustainX smart grid program (U.S. National Energy Technology Laboratory)
[177] Institute of Engineering Thermophysics 2019 Project 'Large scale CAES system R&D and demonstration,' passed inspection (www.etp.ac.cn/xwdt/zhxw/201902/t20190211_5240114.html)
[178] Akhurst M *et al* 2013 Liquid air in the energy and transport systems (The Centre for Low Carbon Futures)
[179] Mongird K, Fotedar V, Viswanathan V, Koritarov V, Balducci P, Hadjerioua B and Alam J 2019 *Energy storage technology and cost characterization report* (Richland, WA: U.S. Department of Energy)
[180] Freund S, Schainker R and Moreau R 2012 Commercial concepts for adiabatic compressed air energy storage *Proc: Renewable Energy Storage Conf.* (*Berlin, Germany*)
[181] Klumpp F 2015 Potential for large scale energy storage technologies—comparison and ranking including an outlook to 2030 *Energy Procedia* **73** 124–35
[182] Abdon A, Zhang X, Parra D, Patel M K and Bauer C 2017 Techno-economic and environmental assessment of stationary electricity storage technologies for different time scales *Energy* **139** 1173–87

[183] Schoenung S 2011 *Energy Storage Systems Cost Update: A Study for the DOE Energy Storage Systems Program* (Livermore, CA: Sandia National Laboratories)
[184] Héder M 2017 From NASA to EU: the evolution of the TRL scale in public sector innovation *Public Sect. Innovation J.* **22** 3
[185] International Energy Association 2020 IEA Energy Storage Annex 36—Carnot Batteries (available at: www.eces-a36.org)
[186] Barnhart C J and Benson S M 2013 On the importance of reducing the energetic and material demands of electrical energy storage *Energy Environ. Sci.* **6** 1083–92
[187] Jenkins S 2020 Economic indicators: CEPCI. Chemical engineering essentials for the CPI professional (www.chemengonline.com/economic-indicators-cepci)
[188] Turton R, Bailie R C, Whiting W B, Shaeiwitz J A and Bhattacharyya D 2012 *Analysis, Synthesis, and Design of Chemical Processes* 4th edn (London: Pearson Education International)
[189] Seider W D, Seider J D, Lewin D R and Widagdo S 2009 *Product and Process Design Principles* 3rd edn (Boston, MA: Wiley)
[190] Couper J R, Penney W R, Fair J R and Walas S M 2012 *Chemical Process Equipment* 3rd edn (Boston, MA: Butterworth-Heinemann)
[191] Valero A, Lozano M A and Serra L 1994 CGAM problem: definition and conventional solution *Energy* **19** 279–86
[192] Schainker R 2008 Compressed air energy storage system cost analysis
[193] Fertig E and Apt J 2011 Economics of compressed air energy storage to integrate wind power: a case study in ERCOT *Energy Policy* **39** 2330–42
[194] Breidenbach N, Martin C, Jockenhöfer H and Bauer T 2016 Thermal energy storage in molten salts: overview of novel concepts and the DLR test facility TESIS *Energy Procedia* **99** 120–9